International Journal of Biological Macromolecules 329 (2025) 147873

Contents lists available at ScienceDirect

International Journal of Biological Macromolecules

journal homepage: www.elsevier.com/locate/ijbiomac

Deacetylase SIRT1 modulates antiviral innate immunity and autoimmune diseases

Shuang-Shuang Yu [1], Hengxiang Yu [1], Shijin Geng, Rong-Chun Tang, Ao Zhang, Yan Zhang, Xiu-Yuan Sun, Jun Zhang [*]

Department of Immunology, School of Basic Medical Sciences, NHC Key Laboratory of Medical Immunology, Medicine Innovation Center for Fundamental Research on Major Immunology-related Diseases, Peking University, Beijing 100191, China

ARTICLE INFO

Keywords:
SIRT1
Innate immunity
Deacetylation
Phosphorylation
IRF3
IRF7

ABSTRACT

Sirtuin 1 (SIRT1), a central NAD^+-dependent deacetylase of the Sirtuin family, has been implicated in immune regulation, yet its role in antiviral signaling remains incompletely understood. Through bioinformatic analysis of GEO datasets, we identified an inverse correlation between *SIRT1* expression and antiviral immune responses. Here, we demonstrate that SIRT1 negatively regulates virus-induced type I interferon (IFN-I) production. Overexpression of SIRT1 attenuated virus-induced IFNβ and ISRE activation, along with diminished IFN-I responses and enhanced viral replication in a deacetylase-dependent manner. Conversely, knockout of SIRT1 potentiates virus-induced IFN-I signaling. Mechanistically, SIRT1 physically interacts with IRF3 and IRF7, deacetylating IRF3 at lysine residues K39/K77 and IRF7 at K92. This post-translational modification impaired the dephosphorylation of IRF3 (S97) and IRF7 (S101/S112) by the phosphatase PTENα, thereby inhibiting their nuclear translocation. Pharmacological inhibition of SIRT1 with EX527 augmented virus-triggered IFN-I responses. Clinically, SIRT1 expression inversely correlated with IFN-I pathway activation in patients with autoimmune diseases (systemic lupus erythematosus, primary Sjögren's syndrome, and dermatomyositis). In *Trex1*-deficient mice, a model of autoimmune disease, SIRT1 activation via Resveratrol or SRT1720 ameliorated pathological phenotypes. Collectively, these findings position SIRT1 as a rheostat for innate immune homeostasis through direct deacetylation of IRF3/IRF7, highlighting its therapeutic potential in viral infections, interferonopathies and autoimmune disorders.

1. Introduction

The innate immune system serves as an evolutionarily conserved defense mechanism against pathogenic invasion. Upon viral infection, pattern recognition receptors (PRRs) play a vital role in detecting viral nucleic acids and initiating an appropriate immune response [1]. Among PRRs, endosomally localized Toll-like receptors (TLRs 3/7/8/9) exhibit remarkable specificity for distinct nucleic acid patterns—double-stranded RNA (TLR3), single-stranded RNA (TLR7/8), and unmethylated CpG DNA (TLR9) [2]. Cytosolic RIG-I-like receptor (RLR) family (RIG-I, MDA5), recognize cytosolic viral RNA. DNA sensors, such as cGAS, IFI16, DDX41, and ZBP1, detect viral DNA in the cytosol or the nucleus [3]. Upon ligand engagement, these receptors initiate signaling cascades through specialized adaptors (TRIF, MyD88, MAVS, or STING), converging on the activation of TANK-binding kinase 1 (TBK1) and IKKε kinases. This culminates in the phosphorylation and dimerization and nuclear translocation of interferon regulatory factor 3 (IRF3) and interferon regulatory factor 7 (IRF7), the master regulators of type I interferon transcription. Concurrently, PRR signaling activates the NF-κB and MAPK pathways, orchestrating a coordinated inflammatory

Abbreviations: SIRT1, Sirtuin 1; IFN, Interferon; ISRE, Interferon-Stimulated Response Element; ISG, Interferon-Stimulated Gene; KO, Knockout; PRR, Pattern recognition receptor; TLR, Toll-like receptors; RLR, RIG-I-like receptor; TBK1, TANK-binding kinase 1; IRF, Interferon regulatory factor; HEK, Human embryonic kidney; SeV, Sendai Virus; GFP, Green fluorescent protein; HSV-1, Herpes Simplex Virus 1; VSV, Vesicular Stomatitis Virus; AID, Autoimmune disease; DM, Dermatomyositis; PSS, Primary Sjögren's syndrome; SLE, Systemic lupus erythematosus; GEO, Gene Expression Omnibus; GSEA, Gene set enrichment analysis; PTM, Post-translational modification; RSVL, Resveratrol.

* Corresponding author.
E-mail address: junzhang@bjmu.edu.cn (J. Zhang).

[1] These authors contributed equally to this work.

https://doi.org/10.1016/j.ijbiomac.2025.147873
Received 29 June 2025; Received in revised form 17 September 2025; Accepted 22 September 2025
Available online 24 September 2025

response [1].

The antiviral innate immune response operates under stringent regulatory constraints to ensure that an effective innate immune response is mounted and to prevent excessive activation that could damage host tissues. Dysregulation of the antiviral innate immune response is closely linked to a number of diseases. An inadequate response can increase the susceptibility to viral infections, while overactivation can lead to chronic inflammation and autoimmune diseases (AIDs) [4].This delicate equilibrium is maintained through multilayered control mechanisms, with recent studies highlighting the critical roles of post-translational modifications, including phosphorylation, ubiquitination, sumoylation, acetylation, *etc.*, in the regulation of antiviral innate immune response [5,6].

Protein acetylation is a reversible post-translational modification that adds an acetyl group to a target protein, typically to the ε-amino group of a lysine residue. Acetylation is catalyzed by enzymes known as lysine acetyltransferases (KATs) and reversed by lysine deacetylases (KDACs). Acetylation can alter gene transcription, protein stability, localization, protein-protein interaction and signal transduction [7]. Acetylation can also interplay with other post-translational modifications such as phosphorylation or ubiquitination, *etc.*, forming combinatorial codes that fine-tune immune responses [8]. The complex regulatory functions of acetylation and deacetylation in innate immunity are widely reported. For example, the DNA sensor cGAS undergoes sophisticated acetylation regulation: basal acetylation at K384/K394/K414 maintains immune quiescence, while N-terminal acetylation at K63 and K83 by KAT5 promoted its DNA-binding ability [9,10]. Furthermore, viral infection triggers the phosphorylation of MYO1F by SYK, which in turn recruits KAT2A to acetylate cGAS at K421, K292 and K131, which facilitates the plasma membrane localization and activation of cGAS [11].

SIRT1, a core member of the class III NAD^+ dependent deacetylases, is widely recognized as an anti-inflammatory deacetylase [12]. In addition to deacetylating histones, a number of non-histone targets have been identified for SIRT1, of which p65 is the major target for SIRT1 to control inflammation [13]. Acetylation of transcription factors, the NF-κB family member p65 at K310 enhanced its DNA binding activity and is critical for its full transcriptional activity. Deacetylation of p65 K310 inhibited the transcriptional activity of p65 and the production of proinflammatory cytokines such as TNF-α and IL-6 in macrophages [14,15]. Growing evidence suggests SIRT1 plays broader roles in immune regulation. Our previous work revealed that SIRT1 modulates interferon responses by deacetylating STAT1/STAT3, thereby fine-tuning JAK-STAT signaling and interferon-stimulated gene (ISG) expression [16].

In this study, initial bioinformatics analysis of influenza infection datasets revealed a significant inverse correlation between SIRT1 expression and type I IFN signaling, promoting investigation of SIRT1's role in antiviral innate immunity. Using gain- and loss-of-function approaches, we demonstrate that SIRT1 suppresses virus-induced type I IFN signaling presumably in a deacetylase-dependent manner. Pharmacological inhibition with EX527 potentiated antiviral responses. SIRT1 activation by agonists (Resveratrol or SRT1720) ameliorated detectable autoimmune phenotypes in *Trex1-KO* mice.

2. Materials and methods

2.1. Cells and viruses

HEK293T, HCT116, 2fTGH-ISRE, Vero, and L929 cells were maintained in DMEM (Thermo-Fisher) supplemented with 10 % heat inactivated FBS (Cellmax, China), 100 U/mL penicillin, and 100 μg/mL streptomycin (Solarbio, China). THP-1 cells were cultured in RPMI 1640 medium (Thermo-Fisher, USA) under the same supplementation conditions. Wild-type (WT) and *SIRT1-knockout* (*SIRT1-KO*) HCT116 cells were kindly provided from Dr. Wei Yu (Fudan University, China). The 2fTGH-ISRE cell line was provided by Dr. Zhengfan Jiang (Peking University, China). *IRF3-KO* HEK293T cell line was provided by Dr. Fuping You (Peking University, China). SeV was propagated in chicken embryos, while VSV, VSV-GFP and HSV-1-GFP were amplified by infecting Vero cells. The viral titers were determined using the TCID50 method on L929 cells.

2.2. Plasmids and transfection

The Myc-tagged SIRT1 plasmid was kindly provided by Dr. Jianyuan Luo (Peking University, China). The plasmids of SIRT1 mutant (H363Y), IRF3 mutants (1-150aa, 151-427aa, K39/77R, S97A) and IRF7 mutants (1-150aa, 151-503aa, 190-503aa, K45R, K50R, K61R, K92R, K120R, S23/24A, S23/24D, S53A, S53D, S73/74A, S73/74D, S101A, S101D, S112A, S112D, S125A, S125D, S101/112A) were constructed using seamless cloning or QuikChange protocol and verified by sequencing. The pRK-Flag-IRF3, pRK-HA-IRF3, pRK-Flag-IRF3-5D, pRK-Flag-IRF7, pRK-HA-IRF7, pRK-Flag-cGAS, pRK-Flag-STING, pRL-SV40, IFNβ, and ISRE luciferase reporter plasmids were kindly provided by Dr. Hong-Bing Shu (Wuhan University, China). The pEF-Bos-Flag-RIG-IN plasmid was kindly provided by Dr. Takashi Fujita (Kyoto University, Japan). The pcDNA-Flag-MAVS plasmid was a kindly gift from Dr. Zhijian J. Chen (University of Texas Southwestern Medical Center, USA). pcDNA-Flag-TBK1 and pcDNA-Flag-IKKε plasmids were kindly gifts from Dr. Tom Maniatis (Columbia University, USA). GFP-PTENα and Flag-PTENα plasmids were kindly gifts from Dr. Dan Lu (Peking University, China). The HA-Ub plasmid was a kindly gift from Dr. Hong Tang (Zhejiang University, China). Plasmids were transfected into HEK293T or HCT116 cells using polyethyleneimine (PEI, Polysciences, USA) according to the manufacturer's instructions.

2.3. Reagents and antibodies

The poly (dA:dT) (tlrl-patn) and poly (I:C) (tlrl-pic) were purchased from InvivoGen. DMSO was obtained from Solarbio. The SIRT1 inhibitor EX527 (S1541) and agonist SRT1720 (S1129) were purchased from Selleck Chemicals. The SIRT1 agonist Resveratrol (RSVL, HY-16561) was from MedChemExpress. GAPDH mAb (M20006S), β-tubulin mAb (M30109S) and HA-tag mAb (M20003S) were from Abmart. Vinculin pAb (4650S) was from Cell Signaling Technology. The Myc-tag mAb (TA150121) was from Origene. Flag-tag mAb (M185-3 L) and GFP pAb (MBL598) antibodies were from MBL. Lamin B1 mAb (66095-1-Ig), SIRT1 pAb (13161-1-AP) and IRF3 pAb (11312-1-AP) were from Proteintech. IRF7 mAb (sc-74471) and phosphoserine (p-Ser) mAb (sc-81514) were from Santa Cruz. Acetylated-lysine mAb (PTM-105RM) was from PTM Biolabs. Control mouse IgG (I5381) and rabbit IgG (I5006) were from Sigma-Aldrich. HRP-conjugated goat anti-mouse IgG (BF03001) and HRP-conjugated goat anti-rabbit IgG (BF03008) were from Biodragon.

2.4. Luciferase assays and type I IFN bioassay

HEK293T cells (2×10^5 cells/ml) were seeded in 24-well plates, and after 24 h, cells were transfected with 1 ng pRL-SV40 plasmid, 100 ng either IFNβ or ISRE luciferase reporter plasmid, and other indicated plasmids, followed by different treatments. Luciferase activity was measured using the Dual-Luciferase Reporter Assay Kit (Promega, USA) according to the manufacturer's instructions. The promoter activity was calculated by dividing the Firefly luciferase (reporter signal) luminescence by the Renilla luciferase signal (internal control).

To assess type I interferon bioactivity, culture supernatant from treated cells were collected and incubated with 2fTGH-ISRE reporter cells for 6 h. Cells were then lysed with 1× passive lysis buffer for 30 min. Cleared lysates were assayed for luciferase activity, and IFN-I bioactivity was quantified based on bioluminescence intensity.

2.5. RT-PCR and quantitative real-time PCR

Total RNA was extracted using TRIzol reagent (Gene-Protein Link, China) according to the manufacturer's protocol. Reverse transcription was performed using the Hifair III 1st Strand cDNA Synthesis Kit (Yeasen, China). Real-time PCR was carried out with the Hieff qPCR SYBR Green Master Mix (Yeasen, China) on the ABI Q5 Detection System. The following gene-specific primers were used:

Human *GAPDH* forward: 5′-ACCCACTCCTCCACCTTTGA-3′, reverse: 5′-CTGTTGCTGTAGCCAAATTCGT-3′; Human *IFNB1* forward: 5′-ACTGCCTCAAGGACAGGATG-3′, reverse: 5′-GGCCTTCAGGTAATGCAGAA-3′; Mouse *β-actin* forward: 5′-AGAGGGAAATCGTGCGTGAC-3′, reverse: 5′-CAATAGTGATGACCTGGCCGT-3′; Mouse *Ifnb1* forward: 5′-CAGCTCCAAGAAAGGACGAAC-3′, reverse: 5′-GGCAGTGTAACTCTTCTGCAT-3′; Mouse *Oas1* forward: 5′-GCCTGATCCCAGAATCTATGC-3′, reverse: 5′-GAGCAACTCTAGGGCGTACTG-3′; Mouse *Cxcl10* forward:5′-GCCGTCATTTTCTGCCTCA-3′, reverse: 5′-CGTCCTTGCGAGAGGGATC-3′; Mouse *Tnf* forward:5′-GGTCCCCAAAGGGATGAGAA-3′, reverse: 5′-TGAGGGTCTGGGCCATAGAA-3′; VSV forward:5′-ACGGCGTACTTCCAGATGG-3′, reverse: 5′-CTCGGTTCAAGATCCAGGT-3′.

2.6. Cytoplasmic and nuclear protein extraction

Cells collected were lysed in cytoplasmic lysis buffer (50 mM Tris-HCl, 100 mM NaCl, 0.05 %NP-40, 1 mM EDTA, 1 mM DTT) on ice for 2–5 min, then centrifuge at 4 °C, 3000 rpm for 5 min, the supernatant was collected for cytoplasmic extracts. The pellet was washed with PBS and subsequently lysed in RIPA lysis buffer (Applygen, China) on ice for 1 h, the supernatant was collected for nuclear extracts.

2.7. Immunoblot analysis

HEK293T, HCT116 or THP-1 cells treated as indicated were collected and lysed in RIPA lysis buffer (Applygen, China) containing protease and phosphatase inhibitors (Roche, Switzerland) on ice for 1 h. The protein concentrations were determined using BCA Quantitative Kit (Beyotime, China). Samples were mixed with 5 × SDS loading buffer, boiled at 100 °C for 10 min, followed by SDS-PAGE. The nitrocellulose filter membrane was blocked with 5 % non-fat powdered milk at room temperature for 1 h, and then incubated with diluted primary antibodies at 4 °C overnight. After washing with TBST, the membranes were incubated with the secondary antibody at room temperature for 1 h and imaged using ImageQuant LAS 500.

2.8. Immunoprecipitation (IP)

HEK293T cells or THP-1 cells treated as indicated were lysed in IP lysis buffer (Beyotime, China) containing protease and phosphatase inhibitors at 4 °C for 1 h. For IP assays, the lysates were additionally boiled at 95 °C for 5 min. After sonicated for 20–30 s, the supernatant was incubated with control IgG or specific antibodies at 4 °C overnight, followed by incubation with Protein A agarose for 3–4 h. The beads were washed for 4–6 times, the beads were resuspended in loading buffer and boiled for 10 min and subject to immunoblot analysis. The protein expression was analyzed with corresponding antibodies. Acetylation or phosphorylation levels were assessed using anti-acetyl-lysine or anti-phosphoserine antibodies(p-Ser), respectively.

2.9. Mice and animal experiments

The *Trex1*$^{+/-}$ mice were kindly provided by Dr. Tomas Lindahl (The Francis Crick Institute, United Kingdom) [17]. *Sirt1*$^{+/-}$ mice were kindly provided by Dr. Michael W. McBurney (University of Ottawa, Canada) [18]. All mice were on the C57BL/6 background and bred under specific pathogen-free conditions. Animal procedures were approved by the Institutional Animal Care and Use Committee of Peking University Health Science Center.

Three to four-week-old female mice of the same age were divided into 3 groups and were intraperitoneally injected DMSO, RSVL (40 μg/g), or SRT1720 (20 μg/g) daily for 2 weeks. Then the hearts were harvested for RT-qPCR and HE staining. WT and *Sirt1*$^{+/-}$ mice were intravenously infected with VSV (5×10^7 pfu/each) for 24 h, then the organs were harvested and detected by RT-qPCR.

2.10. Data analysis of GEO datasets

Gene Expression Omnibus (GEO) datasets GSE100160, GSE65391, GSE61635, GSE135779, GSE84844, and GSE46239 were downloaded from GEO database (https://www.ncbi.nlm.nih.gov/gds). Pearson correlation was used to evaluate relationships between *SIRT1* and *IFNA1/IFNB1*. A pre-ranked gene list based on Pearson's correlation between SIRT1 and other genes was used as input for Gene Set Enrichment Analysis (GSEA). GSEA was conducted and visualized by ClusterProfiler package. Single-cell RNA sequencing (ScRNA-seq) data were processed using Seurat package and the AUCell package was used to identify cells with specific gene sets.

2.11. Statistical analysis

The data were analyzed with GraphPad Prism 9.0. Comparisons between two groups used unpaired two-tailed Student's *t*-tests; multiple groups were compared by ANOVA. Correlation was assessed using Pearson's coefficient. Results are presented as mean ± SD. $P < 0.05$ was considered to be significant.

3. Results

3.1. Negative correlation of SIRT1 with virus-induced type I IFN signaling

To systematically evaluate the relationship between the Sirtuin family members and antiviral immune response we analyzed the transcriptomic data from influenza-infected patients GSE100160. The whole blood RNA sequencing revealed a significant inverse correlation between SIRT1 expression and several IFN-I genes (Fig. 1A). Further GSEA analysis showed that the expression of *SIRT1* was negatively correlated with both IFN-I response and antiviral-related pathways in influenza patients (Fig. 1B&C). These data suggest that the *SIRT1* gene is negatively associated with the RNA virus-induced IFN-I signaling pathway.

To functionally validate the regulatory function of SIRT1 in virus-induced IFN-I signaling, we employed a dual-luciferase reporter gene system to monitor IFNβ and Interferon-Stimulated Response Element (ISRE) reporter activation. It was shown that SIRT1 inhibited IFNβ and ISRE reporter activation induced by RNA virus Sendai Virus (SeV), and this inhibition was dose-dependent (Fig. 1D&E). Besides, SIRT1 reduced the IFNβ and ISRE reporter activation induced by cGAS/STING (Fig. 1F&G), which involved in DNA virus induced IFN-I signaling. Similar phenomenon was observed upon Herpes Simplex Virus 1(HSV-1) infection (data not shown). In addition, we also performed stimulation with RNA virus mimic poly (I:C) and DNA virus mimic poly (dA:dT) and found that SIRT1 exerted similar inhibitory effects (Fig. 1H&I). The above results suggest that SIRT1 broadly inhibits IFN-I signaling pathways, triggered either by RNA virus (RIG-I) or DNA virus (cGAS-STING).

3.2. SIRT1 negatively regulates RNA virus-induced IFN-I expression and promotes viral replication

To further elucidate the role of SIRT1 in virus induced type I IFN production, we examined the effects of SIRT1 overexpression on both the transcription and secretion of type I IFN in response to viral infection. The HEK293T cells were transfected with either a control plasmid, or a SIRT1-expressing plasmid, followed by infection with SeV. Cells and

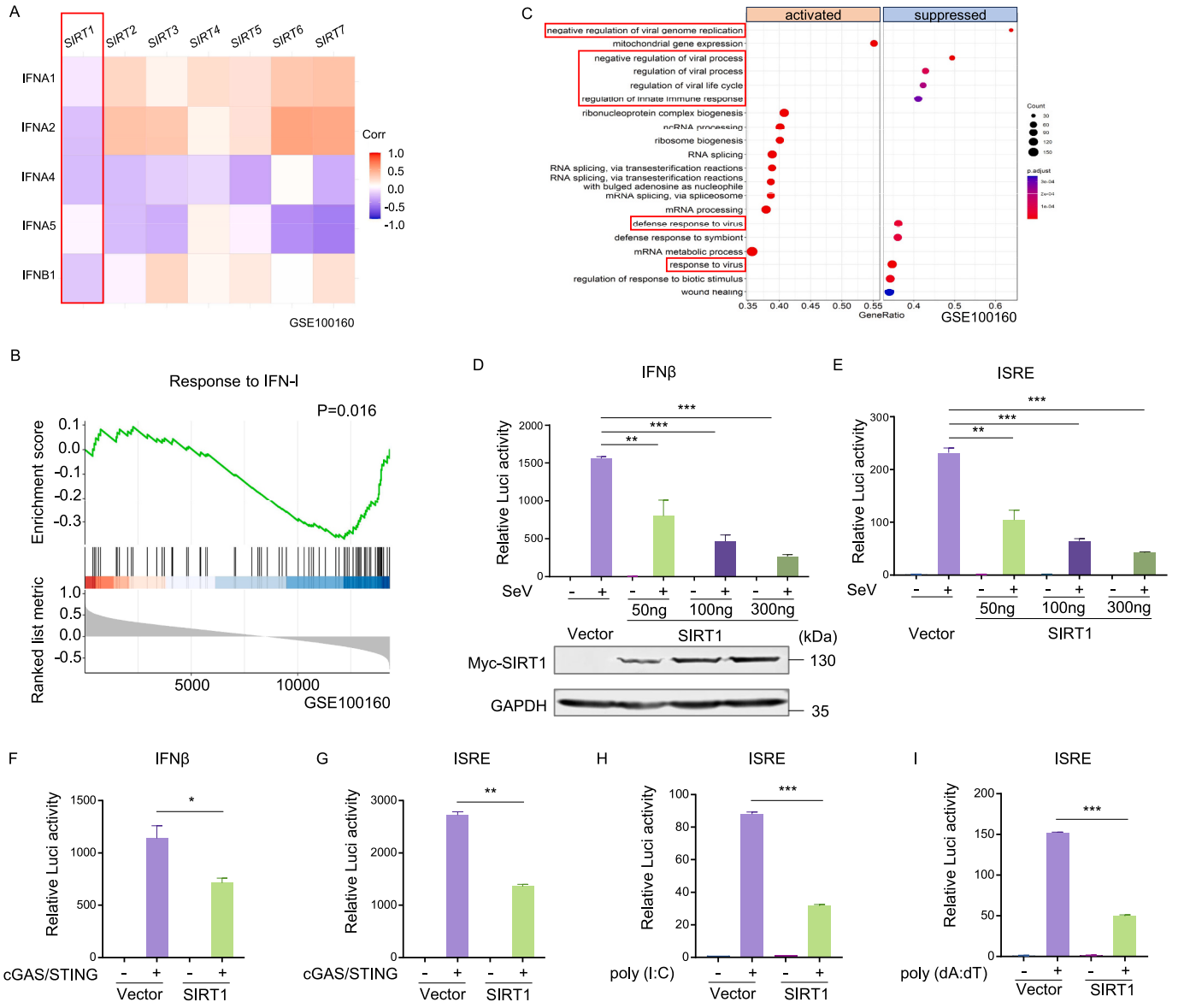

Fig. 1. SIRT1 inhibits the IFN-I pathway. A Correlation between the expression levels of *SIRT1-7* and IFN-I in GSE100160($n = 39$). B&C Analysis of the correlation between SIRT1 and the IFN-I (B) /virus related pathways (C) through gene set enrichment analysis (GSEA) in GSE100160. D&E Luciferase activity analysis of the IFNβ (D)/ISRE (E) reporter in human embryonic kidney (HEK) 293 T cells transfected with a control vector or SIRT1 expressing plasmid and then infected with SeV (MOI = 1) for 24 h. F&G Luciferase activity analysis of IFNβ (F)/ISRE (G) reporter in HEK293T cells transfected with control vector or SIRT1 expressing plasmid cotransfected with Flag-cGAS/STING for 24 h. H&I Luciferase activity analysis of the IFNβ (H)/ISRE (I) reporter in HEK293T cells transfected with a control vector or SIRT1 expressing plasmid and then transfected with poly (I:C) or poly (dA:dT) for 24 h. (*$P < 0.05$, **$P < 0.01$, ***$P < 0.001$.)

culture supernatants were collected at various time points post-infection. Overexpression of SIRT1 significantly suppressed SeV-induced *IFNB1* expression compared to the control (Fig. 2A). To assess the bioactivity of type I IFN in the supernatants, we employed 2fTGH-ISRE cells–a reporter cell line stably expressing and ISRE-driven luciferase gene. Consistent with the transcriptional data, overexpression of SIRT1 markedly reduced SeV-induced type I production (Fig. 2B). We further evaluated whether viral infection alters SIRT1 expression. Infection with either SeV or HSV-1 in HEK293T cells, HCT116, and THP-1 cells did not affect SIRT1 protein levels (data not shown). To determine the functional consequence of SIRT1 in viral infection, we monitored the RNA viral replication of Vesicular Stomatitis Virus (VSV)-GFP infection in SIRT1 overexpression cells using WB, real-time PCR, or fluorescence microscopy. SIRT1 overexpression enhanced VSV replication (Fig. 2C-E), supporting its role in attenuating antiviral IFN responses.

To investigate the effects of endogenous SIRT1 on type I IFN production and viral replication, the WT/*SIRT1-KO* HCT116 cell line constructed by CRISPR-Cas9 technology was validated and used for further studies (Fig. 2F). WT or *SIRT1-KO* HCT116 cells were infected with SeV, after which the cells and culture supernatants were collected at various time points to assess the expression of downstream target genes *IFNB1*. As shown in Fig. 2G, *SIRT1* knockout significantly enhanced SeV-induced *IFNB1*expression compared to the WT control. Using 2fTGH-ISRE reporter cells to evaluate the bioactivity of type I IFN in supernatants, we observed that SIRT1 knockout markedly increased SeV-induced IFN-I production (Fig. 2H).

To extend these findings in a physiological model, we employed *Sirt1*$^{+/-}$ mice, as *Sirt1*$^{-/-}$ mice exhibit embryonic and postnatal developmental defects [18]. Primary peritoneal macrophages from *Sirt1*$^{+/-}$ mice showed elevated *Ifnb1* expression upon SeV infection compared to those from WT mice (Fig. 2I). We further evaluated antiviral responses

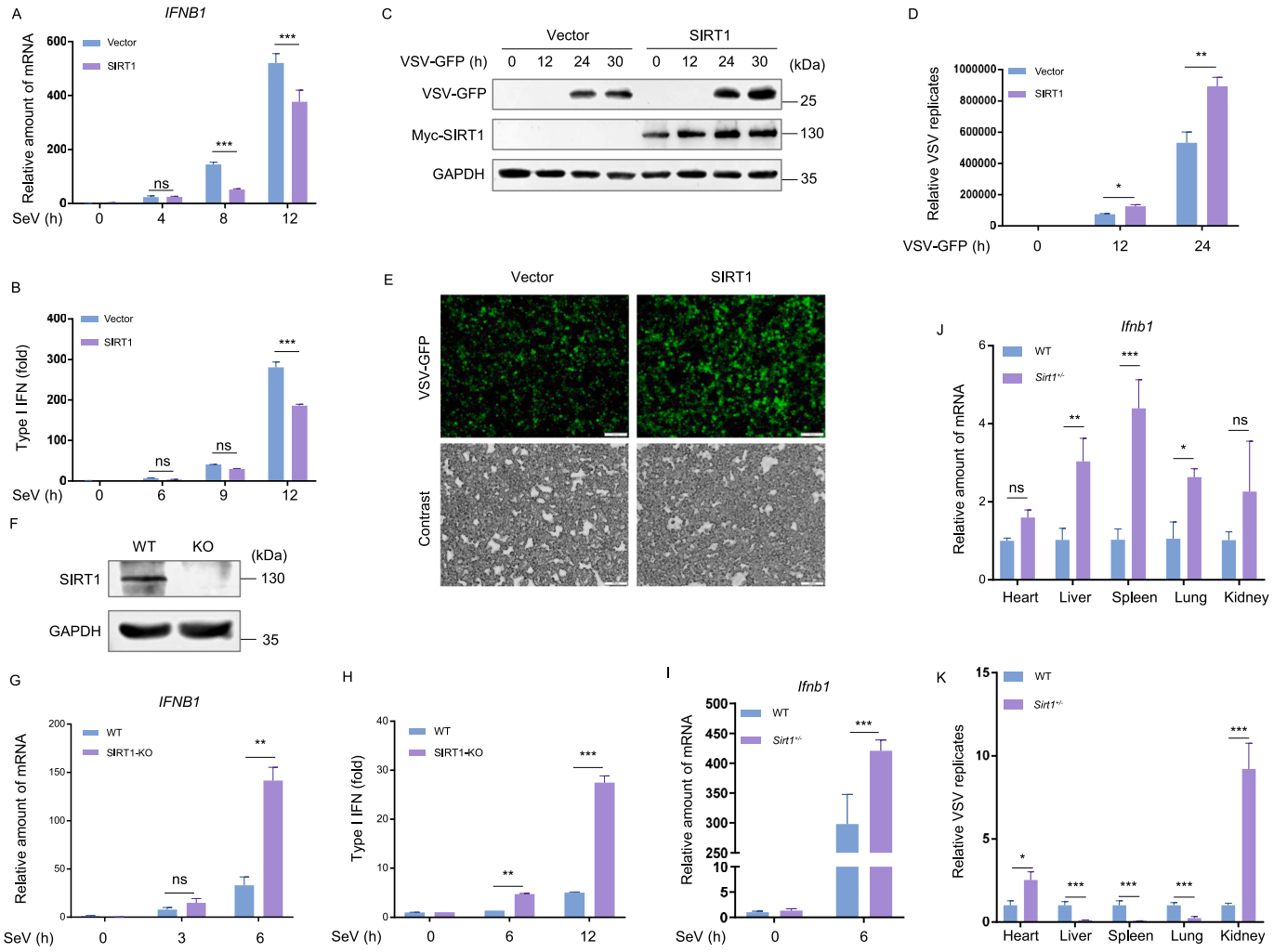

Fig. 2. SIRT1 negatively regulates RNA-virus induced IFN expression and promotes viral replication. A RT-qPCR analysis of *IFNB1* mRNA in HEK293T cells transfected with control vector or SIRT1 expressing plasmid and then infected with SeV (MOI = 1) for indicated time points. B HEK293T cells transfected with a control vector or SIRT1 expressing plasmid and then infected with SeV (MOI = 1), cell culture supernatants were collected at different time points and the activity of IFN-I were detected 2fTGH-ISRE cells. C-E HEK293T cells transfected with control vector or SIRT1 expressing plasmid were infected with VSV-GFP (MOI = 1) for 24 h, then detected by immunoblot (C), RT-qPCR (D), and fluorescence analysis (E). F Immunoblot analysis of SIRT1 in WT and *SIRT1-KO* HCT116 cell line. G RT-qPCR analysis of *IFNB1* mRNA in WT and *SIRT1-KO* HCT116 cells infected with SeV (MOI = 1) for indicated time points. H WT and *SIRT1-KO* HCT116 cells infected with SeV (MOI = 1), cell culture supernatants were collected at different time points, and the activity of IFN-I was detected in 2fTGH-ISRE cells. I RT-qPCR analysis of Ifnb1 mRNA in WT and *Sirt1*$^{+/-}$ primary peritoneal macrophages infected with SeV (MOI = 1). J-K WT and *Sirt1*$^{+/-}$ mice (n = 3 per group) were infected with VSV (5×10^7 pfu, i.v.) for 24H, Ifnb1 mRNA (J) and relative VSV replicates (K) in the organs were analyzed with RT-qPCR. (Scale bars, 100 μm. *$P < 0.05$, **$P < 0.01$, ***$P < 0.001$.)

in vivo by intravenously infecting mice with VSV for 24 h, and analyzing the organ samples. *Sirt1*$^{+/-}$ mice exhibited higher *Ifnb1* expression levels, and VSV replication was significantly suppressed in liver, spleen and lung relative to WT controls (Fig. 2J&K). Collectively, these results demonstrate again that SIRT1 acts as a negative regulator in virus-induced type I IFN signaling.

3.3. SIRT1 targets IRF3 and IRF7

To identify the molecular targets through which SIRT1 regulates virus-induced type I IFN signaling cascade, we systematically evaluated its effects on key components of the IFN pathway using IFNβ and ISRE reporter luciferase reporter assays. HEK293T cells were co-transfected with SIRT1 and RIG-IN (activated form of RIG-I)/MAVS/TBK1/IKKε/IRF3-5D (activated form of IRF3)/IRF7. SIRT1 dose-dependently inhibited RIG-IN/MAVS/TBK1/IKKε/IRF3-5D/IRF7 induced IFNβ and ISRE reporter activation (Fig. 3A&B), suggesting that SIRT1 acts at the level of or downstream of IRF3 and IRF7. We next examined whether SIRT1 physically interacts with IRF3 or IRF7. Coimmunoprecipitation assays confirmed that SIRT1 interacted with both IRF3 and IRF7 (Fig. 3C). Domain mapping revealed that SIRT1 interacted with the N-terminal domain (1-150aa) of both IRF3 and IRF7 (Fig. 3D-G). Furthermore, endogenous associations between SIRT1 and IRF3 and IRF7 were validated in THP-1 cells, with the interaction between SIRT1 and IRF7 being enhanced following infection with SeV or HSV-1 (Fig. 3H-K). Taken together, these findings suggest that SIRT1 may directly target IRF3 and IRF7 to inhibit virus-induced type I IFN signaling and attenuate antiviral responses.

3.4. SIRT1 deacetylates IRF3

Given that SIRT1 is a well-known deacetylase, we sought to test whether its inhibitory effect on virus-induced type I IFN signaling depend on its enzymatic activity. Previous studies have shown that the H363Y mutation abolishes the deacetylase activity of SIRT1 [19]. To test this, we transfected *SIRT1-KO* HCT116 cells with the control vector,

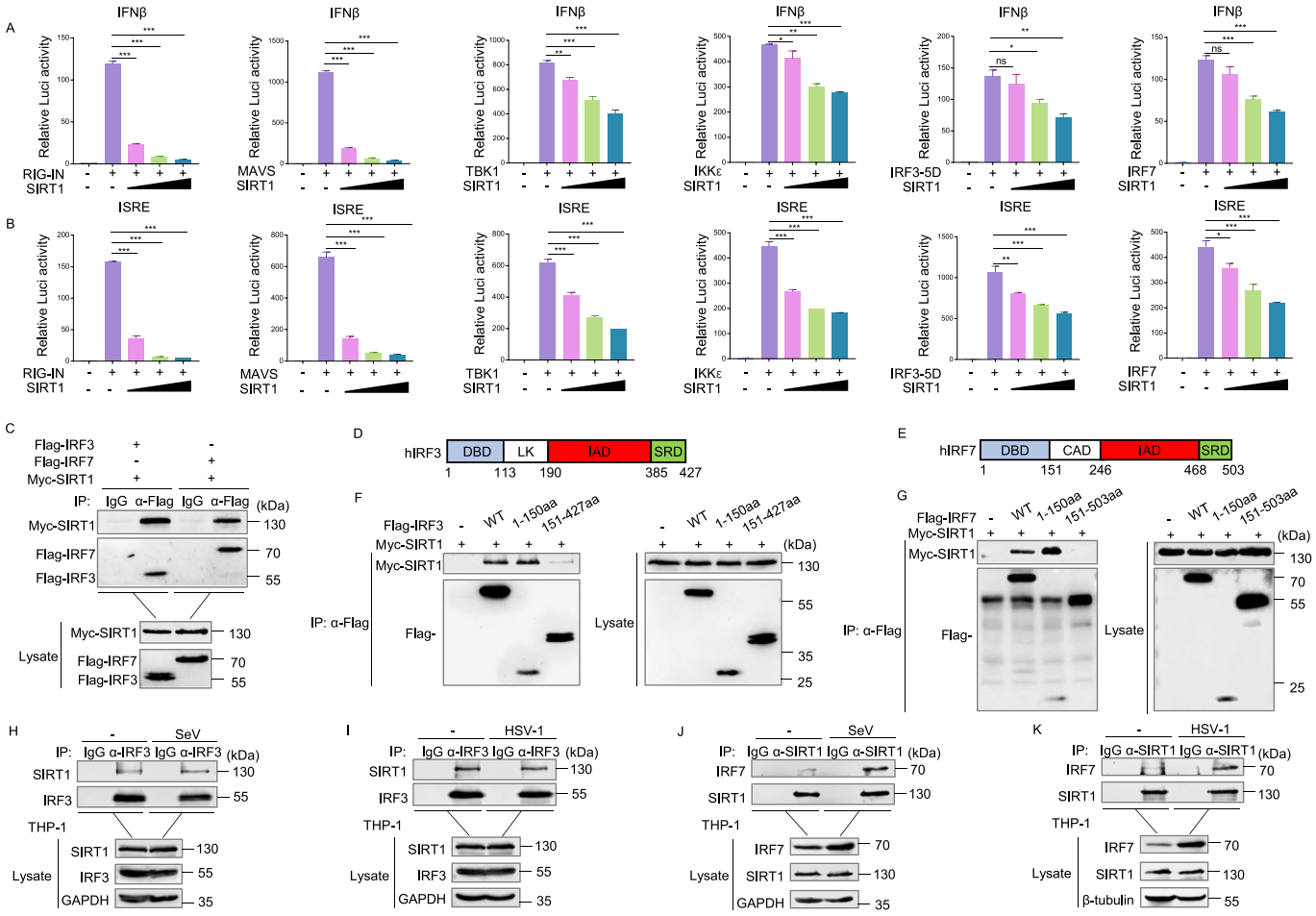

Fig. 3. SIRT1 targets IRF3/IRF7. A&B Luciferase activity analysis of the IFNβ (A)/ISRE (B) reporter in HEK293T cells transfected with a control vector or RIG-IN/MAVS/TBK1/IKKε/IRF3-5D/IRF7 expressing plasmid for 24 h. C Co-immunoprecipitation analysis of the interaction of Myc-SIRT1 with Flag-IRF3 and Flag-IRF7 in HEK293T cells. D&E Structure domains of human IRF3 (D) and IRF7 (E). DBD, DNA binding domain; CAD, constitutive activation domain; VAD, virus-activated domain; ID, inhibitory domain; SRD, signal response domain (serine-rich domain); LK, linker region. F&G Co-immunoprecipitation analysis of HEK293T cells transfected with plasmids encoding Myc-SIRT1 and Flag-IRF3 (F)/Flag-IRF7 (G) or its truncation mutants for 24 h. H-K Co-immunoprecipitation analysis of the interaction of endogenous SIRT1 with IRF3 and IRF7 in THP-1 cells, uninfected (left) or infected (right) with SeV (MOI = 1, H&J) or HSV-1 (MOI = 10, I&K) for 8 h. (*$P < 0.05$, **$P < 0.01$, ***$P < 0.001$.)

SIRT1 WT or SIRT1 H363Y, and measured activation of IFNβ and ISRE reporter following SeV infection. SIRT1 WT significantly suppressed SeV-induced IFNβ and ISRE reporter activation, whereas the SIRT1 H363Y mutant lost most of this inhibitory capacity (Fig. 4A&B). To further confirm the dependence on deacetylase activity, we treated cells with EX527—a highly specific SIRT1 inhibitor with a favorable clinical safety profile [20]. EX527 treatment alleviated the suppressive effect of SIRT1 on SeV-induced activation of IFNβ and ISRE reporters (Fig. 4C&D). Together, these results demonstrate that SIRT1 inhibits virus-induced type I IFN signaling dependent on its deacetylase activity.

We next asked whether SIRT1 deacetylates IRF3. Overexpression of SIRT1 reduced IRF3 acetylation levels (Fig. 4E), and inhibition of SIRT1 with EX527 increased IRF3 acetylation levels (Fig. 4F), confirming that SIRT1 promotes IRF3 deacetylation.

The above data showed that SIRT1 interacted with the N-terminal domain of IRF3 (1-150aa), and then we tried to determine the deacetylation site on IRF3. Using the ASEB (http://bioinfo.bjmu.edu.cn/huac/predict_p/) online prediction tool, we identified K39 and K77 as the most likely acetylation sites within the N-terminal domain. Multiple sequence alignment via Clustal Omega (https://www.ebi.ac.uk/Tools/msa/clustalo) confirmed that both residues are highly conserved across species, including human, bovine, porcine, rat, and mouse (Fig. S1A). To functionally validate these sites, we generated an IRF3 mutant in which both lysines were substituted with arginine (K39/77R). The acetylation level of IRF3 K39/77R was significantly reduced and was no longer responsive to SIRT1-mediated deacetylation (Fig. 4G), indicating that SIRT1 targets IRF3 primarily at K39 and K77 to promote its deacetylation.

3.5. SIRT1 deacetylates IRF7

Building on the findings that SIRT1 interacts with IRF7 and inhibits its transcriptional activity, we sought to determine whether SIRT1 modulates the acetylation status of IRF7. Overexpression of SIRT1 reduced the acetylation level of IRF7 (Fig. 4H). Conversely, treatment with the SIRT1-specific inhibitor EX527 increased IRF7 acetylation (Fig. 4I). Since SIRT1 interacted with the N-terminal domain of IRF7 (1-150aa), we focused on the lysine within this region. Multiple sequence alignment using Clustal Omega revealed that five lysine sites (K45, K92, K120, K128, and K133) are highly conserved across species, including human, bovine, pig, rat, and mouse (Fig. S1B). To identify which of these residues is functionally targeted by SIRT1, we constructed a series of lysine-to-arginine (KR) mutants and assessed their ability to activate an IFNβ reporter. The IRF7 K92R mutant abolished the ability to activate the reporter, while K45R and K120R mutants exhibited reduced activation (Fig. 4J). We then measured acetylation levels of these mutants

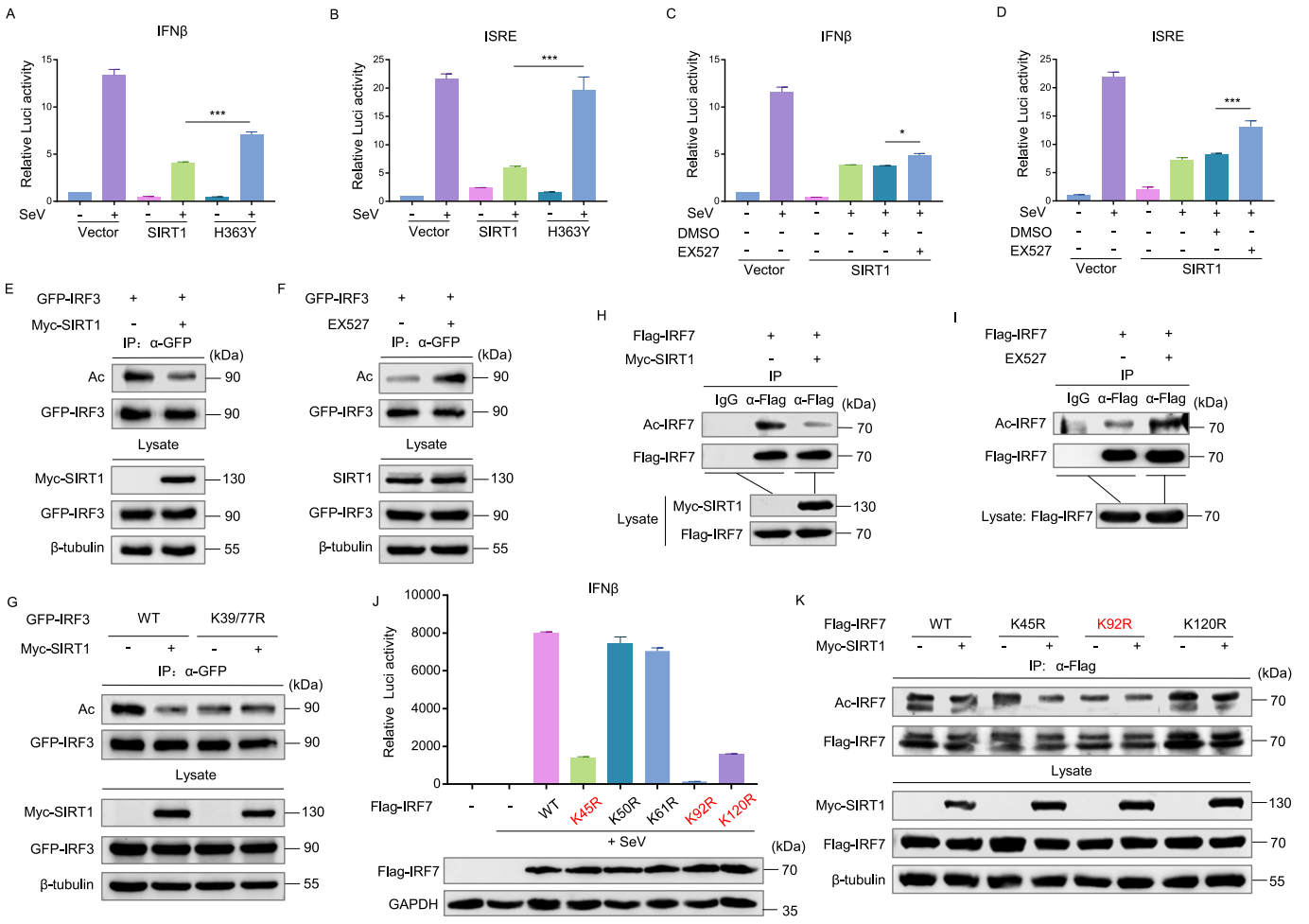

Fig. 4. SIRT1 deacetylates IRF3/IRF7. A&B Luciferase activity analysis of IFNβ/ISRE reporter in *SIRT1-KO* HCT116 cells transfected with control vector or Myc-SIRT1 WT/H363Y expressing plasmid, and then infected with SeV (MOI = 1) for 24 h. C&D Luciferase activity analysis of IFNβ/ISRE reporter in *SIRT1-KO* HCT116 cells transfected with control vector or Myc-SIRT1 WT/H363Y expressing plasmid treated with DMSO or EX527(10 μmol/L)for 4 h, and then infected with SeV (MOI = 1) for 24 h. E Immunoprecipitation analysis of IRF3 acetylation in HEK293T cells transfected with plasmids encoding GFP-IRF3 and Vector or Myc-SIRT1 for 24 h, then infected with SeV (MOI = 1) for 8 h. F Immunoprecipitation analysis of IRF3 acetylation in HEK293T cells transfected with plasmids encoding GFP-IRF3 and then treated with DMSO or EX527 (20 μmol/L) for 2 h, then infected with SeV (MOI = 1) for 8 h. G Immunoprecipitation analysis of IRF3 acetylation in HEK293T cells transfected with plasmids encoding GFP-IRF3 WT or K39/77R and control vector or Myc-SIRT1 for 24 h, then infected with SeV (MOI = 1) for 8 h. H Immunoprecipitation analysis of IRF7 acetylation in HEK293T cells transfected with plasmids encoding Flag-IRF7 and Vector or Myc-SIRT1, and then infected with SeV (MOI = 1) for 24 h. I Immunoprecipitation analysis of IRF3 acetylation in HEK293T cells transfected with plasmids encoding Flag-IRF7 and then treated with DMSO or EX527 (20 μmol/L) for 2 h, then infected with SeV (MOI = 1) for 8 h. J Luciferase activity analysis of IFNβ reporter in IRF3-KO HEK293T cells transfected with control vector or Flag-IRF7 WT/mutant expressing plasmid for 24 h, and then infected with SeV (MOI = 1) for 24 h. K Immunoprecipitation analysis of IRF7 acetylation in HEK293T cells transfected with plasmids encoding Flag-IRF7 WT/mutant and Vector or Myc-SIRT1 for 24 h, and then infected with SeV (MOI = 1) for 8 h. (*$P < 0.05$, ***$P < 0.001$.)

and found that the K92R mutation markedly decreased IRF7 acetylation and abolished responsiveness to SIRT1-mediated deacetylation (Fig. 4K). These results indicate that K92 is the primary deacetylation site through which SIRT1 negatively regulates IRF7 activity.

3.6. SIRT1 enhances the phosphorylation of IRF3 at S97

It is well documented that acetylation can crosstalk with other post-translational modifications, such as phosphorylation [8]. We therefore hypothesized that SIRT1-mediated deacetylation of the effect of IRF3 at K39/K77 sites might influence the phosphorylation status of its N-terminal region. While phosphorylation at its C-terminal serines (S386 and S396) is known to be critical for its full activation [21], less is known about N-terminal phosphorylation events, with only S97 phosphorylation having been reported to regulate nuclear translocation [22].

Due to the lack of commercially available antibodies targeting N-terminal phospho-sites of IRF3, we employed immunoprecipitation followed by immunoblotting with a pan-phosphoserine antibody. Inhibition of SIRT1 with EX527 reduced serine phosphorylation of full-length IRF3 (Fig. 5A), suggesting that SIRT1 activity promotes phosphorylation in this region.

Given that SIRT1 binds and deacetylates the N-terminus of IRF3, we sought to determine whether it specifically enhances phosphorylation within this domain. As the expression of N-terminal IRF3 fragments was too weak to detect the phosphorylation band, we analyzed a C-terminal truncation mutant (amino acids 151–427) instead. EX527 treatment did not affect serine phosphorylation of this fragment (Fig. 5B), indirectly indicating that SIRT1 specifically enhances the phosphorylation within the N-terminal domain of IRF3.

We next examined whether SIRT1 influences the interaction between IRF3 and PTENα—a phosphatase known to dephosphorylate IRF3 at S97 [22]. Co-immunoprecipitation confirmed that PTENα binds the N-terminal region of IRF3 (Fig. 5C). When SIRT1 was co-expressed with IRF3 and PTENα, it significantly disrupted the PTENα–IRF3 interaction

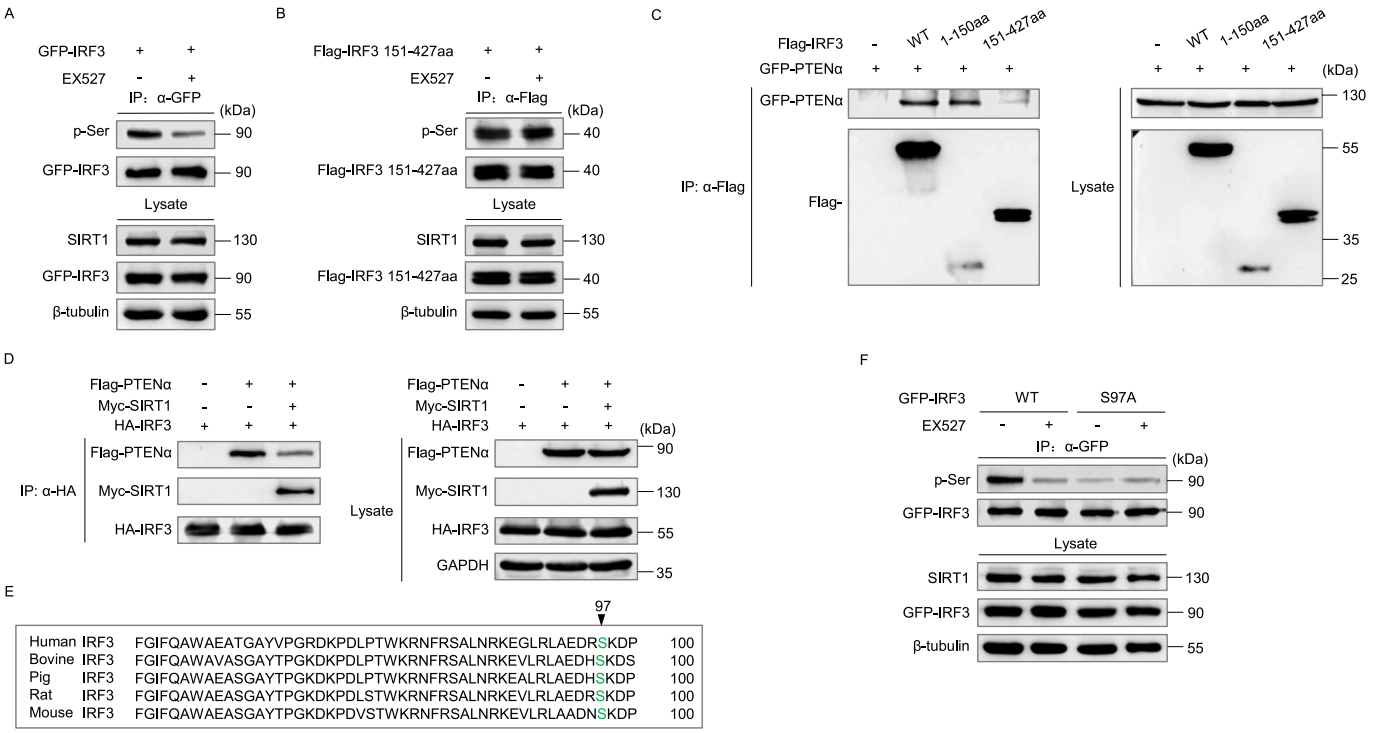

Fig. 5. SIRT1 promotes the phosphorylation of IRF3. A Immunoprecipitation analysis of IRF3 phosphorylation in HEK293T cells transfected with plasmids encoding GFP-IRF3 for 24 h and then treated with DMSO or EX527 (20 μmol/L) for 10 h. B Immunoprecipitation analysis of IRF3 phosphorylation in HEK293T cells transfected with plasmids encoding Flag-IRF3 151-427aa for 24 h and then treated with DMSO or EX527 (20 μmol/L) for 2 h, then infected with SeV (MOI = 1) for 8 h. C Co-immunoprecipitation analysis of HEK293T cells transfected with plasmids encoding GFP-PTENα and Flag-IRF3 or its truncation mutants for 36 h. D Co-immunoprecipitation analysis of HEK293T cells transfected with plasmids encoding GFP-PTENα, HA-IRF3 and Myc-SIRT1 for 36 h. E Sequence conservation analysis of N-terminal serine in IRF3. F Immunoprecipitation analysis of IRF3 phosphorylation in HEK293T cells transfected with plasmids encoding GFP-IRF3 WT/S97A for 24 h and then treated with DMSO or EX527 (20 μmol/L) for 10 h.

(Fig. 5D). This effect was not observed with the catalytically inactive SIRT1 H363Y mutant (Fig. S2A), indicating that SIRT1's deacetylase activity is required for this effect. To assess whether SIRT1 modulates the phosphorylation of IRF3 at S97, we generated an IRF3 S97A mutant. Sequence alignment confirmed that S97 is highly conserved across species (Fig. 5E). EX527 treatment reduced phosphorylation of WT IRF3, whereas the S97A mutant exhibited low baseline phosphorylation that was unaltered by SIRT1 inhibition (Fig. 5F). These results suggest that SIRT1 enhances phosphorylation at S97 by disrupting PTENα-mediated dephosphorylation.

3.7. SIRT1 enhances the phosphorylation of IRF7 at S101/S112

While phosphorylation of IRF7 has been primarily characterized at its C-terminal region [23], the potential N-terminal phosphorylation sites remain unexplored. We therefore investigated whether SIRT1 influences phosphorylation within the N-terminal domain of IRF7. Similar to IRF3, due to the absence of commercial antibodies targeting N-terminal phospho-sites, we employed immunoprecipitation followed by immunoblotting with a pan-phosphoserine antibody. Treatment with EX527 reduced the phosphorylated IRF7 (Fig. 6A). Given our findings that SIRT1 binds and deacetylates the N-terminus of IRF7, we next asked whether it specifically enhances phosphorylation within this region. As expression of N-terminal IRF7 fragments was too weak to detect the phosphorylation band, we analyzed a C-terminal truncated mutant (amino acids 190–503) instead. EX527 treatment did not alter the phosphorylation level of this fragment (Fig. 6B), indirectly indicating that SIRT1 specifically enhances phosphorylation within the N-terminal domain of IRF7.

Based on our earlier finding that SIRT1 disrupts the interaction between PTENα and IRF3—leading to increased IRF3 S97 phosphorylation—we asked whether a similar mechanism operates for IRF7. Domain mapping confirmed that PTENα interacted with the N-terminal region (1–150 aa) of IRF7 (Fig. 6C). Furthermore, PTENα overexpression reduced phosphorylation of full-length IRF7 but not the C-terminal fragment (190–503 aa) (Fig. 6D&E), indicating that PTENα dephosphorylates the N-terminal domain of IRF7. Consistent with observations in IRF3, SIRT1 inhibited the interaction between PTENα and IRF7 (Fig. 6F), whereas, SIRT1 H363Y mutation abolished this effect (Fig. S2B).

To identify specific phospho-sites regulated by SIRT1 in the N-terminal region of IRF7 (1–150 aa), which contains eight serine residues (Fig. 6G), we constructed a series of phospho-defective (SA) and phospho-mimetic (SD) mutants. Reporter assays revealed that IRF7 S101D and S112D mutants significantly suppressed IFNβ activation compared to IRF7 WT (Fig. 6H), suggesting that phosphorylation at these sites negatively regulates type I IFN signaling—a function analogous to that of phosphorylated IRF3 S97. Conservation analysis confirmed that S101 and S112 are highly conserved across species (Fig. 6G).

We then evaluated whether SIRT1 modulates phosphorylation at these sites. EX527 reduced phosphorylation of IRF7 WT and single S101A or S112A mutant, but had no effect on the double mutant IRF7 S101A/S112A (Fig. 6I), indicating that SIRT1 enhances phosphorylation specifically at S101 and S112. Notably, structural alignment revealed that IRF7 S112 is functionally equivalent to IRF3 S97 (Fig. 6J). Together, these results demonstrate that SIRT1 promotes phosphorylation of IRF7 at S101 and S112, likely by disrupting PTENα-mediated dephosphorylation, thereby reinforcing its role as a negative regulator of type I IFN signaling.

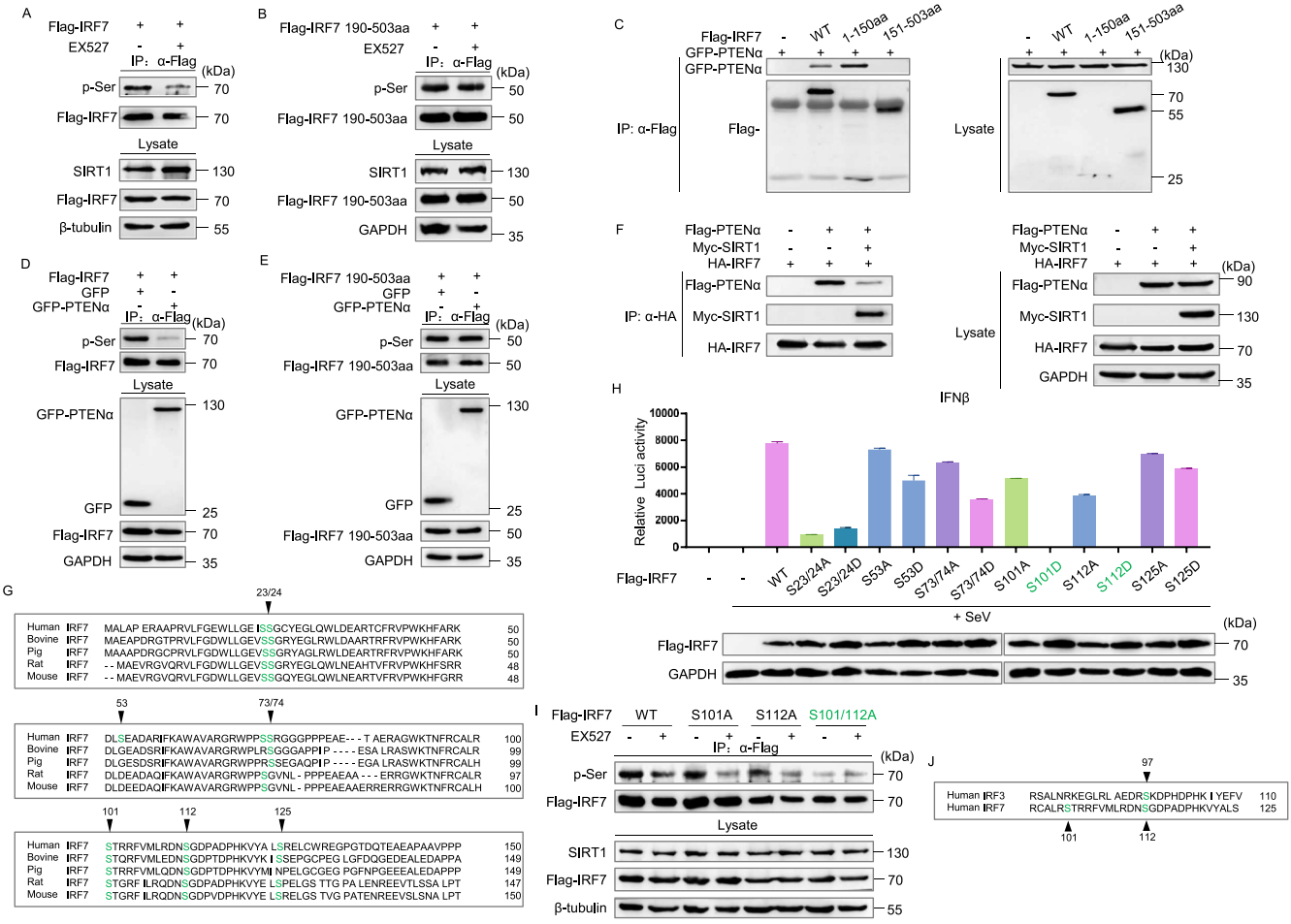

Fig. 6. SIRT1 promotes the phosphorylation of IRF7. A Immunoprecipitation analysis of IRF7 phosphorylation in HEK293T cells transfected with plasmids encoding Flag-IRF7 for 24 h and then treated with DMSO or EX527 (20 μmol/L) for 10 h. B Immunoprecipitation analysis of IRF7 phosphorylation in HEK293T cells transfected with plasmids encoding Flag-IRF7 190-503aa for 24 h and then treated with DMSO or EX527 (20 μmol/L) for 2 h, then infected with SeV (MOI = 1) for 8 h. C Co-immunoprecipitation analysis of HEK293T cells transfected with plasmids encoding GFP-PTENα, Flag-IRF7 or its truncation mutants for 36 h. D&E Immunoprecipitation analysis of IRF7 phosphorylation in HEK293T cells transfected with plasmids encoding Flag-IRF7 WT (D)/190-503aa (E) and GFP-PTENα or GFP 36 h. F Co-immunoprecipitation analysis of HEK293T cells transfected with plasmids encoding GFP-PTENα, HA-IRF7 and Myc-SIRT1 for 36 h. G Sequence conservation analysis of N-terminal serine in IRF7. H Luciferase activity analysis of the IFNβ reporter in *IRF3-KO* HEK293T cells transfected with a control vector or Flag-IRF7 WT/mutant expressing plasmid for 24 h, and then infected with SeV (MOI = 1) for 24 h. I Immunoprecipitation analysis of IRF7 phosphorylation in HEK293T cells transfected with plasmids encoding GFP-IRF3 WT/S97A for 24 h and then treated with DMSO or EX527 (20 μmol/L) for 10 h. J Sequence conservation analysis of N-terminal serine in human IRF3 and IRF7.

3.8. SIRT1 inhibits the nuclear translocation of IRF3 and IRF7

Acetylation modulates diverse physiological activities by affecting dimerization, ubiquitination, and phosphorylation [24]. In addition to its effects on phosphorylation, we asked whether SIRT1 influences the dimerization or ubiquitination of IRF3 and IRF7. The dimerization status of IRF3 and IRF7 was not altered following SIRT1 overexpression (Fig. 7A&B). Similarly, SIRT1 had no effect on the ubiquitination level of IRF3 or IRF7 as well (Fig. S3A&B).

Previous studies have shown that the phosphatase PTENα dephosphorylates IRF3 at S97, thereby promoting its nuclear translocation and enhancing antiviral innate immunity [22]. Although the role of N-terminal phosphorylation of IRF7 in nuclear translocation has not been reported, we found that PTENα also facilitated the nuclear translocation of IRF7 in SeV-infected HEK293T cells (Fig. 7D), mirroring its effect on IRF3 (Fig. 7C). In contrast, PTENα did not promote the nuclear translocation of IRF7 S101/112D (Fig. 7E), indicating that phosphorylation at these N-terminal sites may inhibit nuclear accumulation.

We next evaluated whether SIRT1 influences the nuclear translocation of IRF3 and IRF7. In *SIRT1-KO* HCT116 cells infected with SeV, endogenous IRF3 and IRF7 exhibited significantly enhanced nuclear translocation compared to WT controls (Fig. 7F), consistent with SIRT1's role in promoting inhibitory phosphorylation at N-terminal sites. Together, these results demonstrate that SIRT1 negatively regulates antiviral innate immunity by impeding the nuclear translocation of IRF3 and IRF7—a mechanism dependent on its promotion of N-terminal phosphorylation and disruption of PTENα-mediated dephosphorylation, rather than through effects on dimerization or ubiquitination.

3.9. SIRT1 is negatively correlated with type I interferon signaling in autoimmune diseases

An imbalanced innate immune homeostasis is known to contribute to chronic inflammation and autoimmune diseases [4]. To explore the potential relationship between SIRT1 and type I interferon in autoimmune diseases, we analyzed transcriptomic data from patients with systemic lupus erythematosus (SLE), primary Sjögren's syndrome (PSS), and dermatomyositis (DM), using four independent GEO datasets (GSE65391, GSE61635, GSE84844, and GSE46239).

A consistent negative correlation was observed between SIRT1

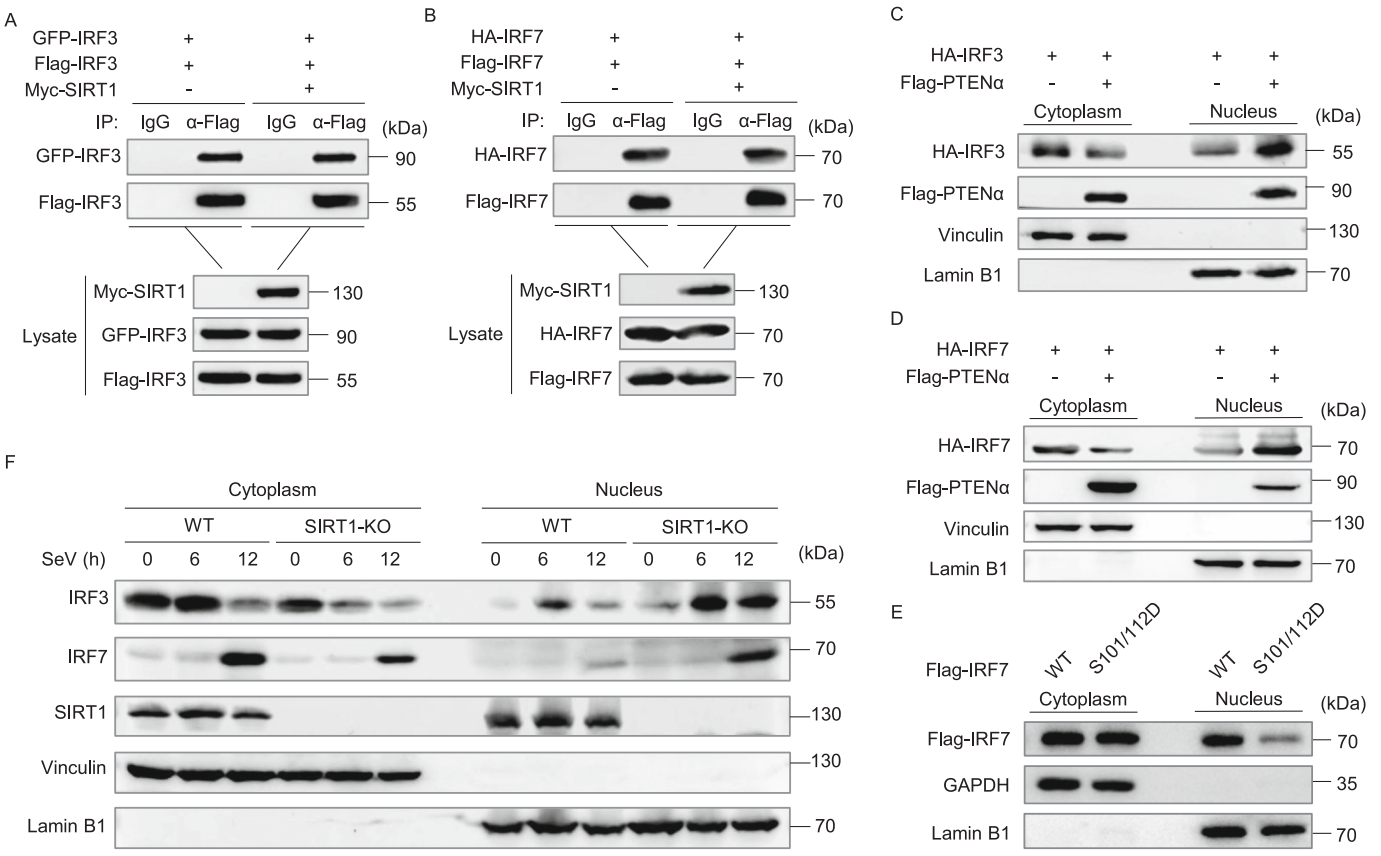

Fig. 7. SIRT1 inhibits nuclear translocation of IRF3 and IRF7. A Co-immunoprecipitation analysis of HEK293T cells transfected with plasmids encoding Flag-IRF3 and GFP-IRF3 for 24 h, and then infected with SeV (MOI = 1) for 8 h. B Co-immunoprecipitation analysis of HEK293T cells transfected with plasmids encoding Flag-IRF7 and HA-IRF7 for 24 h, and then infected with SeV (MOI = 1) for 8 h. C&D Cytosolic and nuclear fractions were extracted from HEK293T cells transfected with plasmids encoding HA-IRF3 (C)/HA-IRF7 (D), and Flag-PTENα for 24 h, then infected with SeV (MOI = 1) for 12 h. E Cytosolic and nuclear fractions were extracted from HEK293T cells transfected with plasmids encoding Flag-IRF7 WT/S101/112D, then infected with SeV (MOI = 1) for 12 h. F Cytosolic and nuclear fractions were extracted from WT and *SIRT1-KO* HCT116 cells infected with SeV (MO I = 1) for the indicated time points. Immunoblotted by indicated antibodies.

expression and levels of *IFNA1/IFNB1* across all AID cohorts (Fig. 8A–D). Given the well-established role of IFN-I in autoimmune pathogenesis [25], we further evaluated the relationship between SIRT1 and IFN-I–driven inflammatory responses. SIRT1 expression was inversely correlated with IFN-I signature scores and general inflammatory response in AID patients (Fig. 8E-H).

To further explore the role of SIRT1 in autoimmune diseases at a higher resolution, we analyzed ~132 k PBMCs from 8 adult SLE patients and 6 matched controls (GSE135779, Fig. 8I). SIRT1 expression was significantly reduced in both $CD4^+$ and $CD8^+$ T cells from SLE patients compared to controls (Fig. 8J). Moreover, SIRT1 levels negatively correlated with IFN-I response gene signatures in these patients (Fig. 8K). Together, these clinical and bioinformatic findings suggest that SIRT1 may serve as an important regulator in the development and modulation of autoimmune diseases, potentially through the suppression of pathogenic IFN-I signaling.

3.10. SIRT1 agonists attenuate the spontaneous autoimmune phenotypes in Trex1-KO mice

It is well-known that mutations in *Trex1* are associated with excessive type I interferon signaling and interferonopathies, often leading to spontaneous autoimmune diseases [26–28]. *Trex1* deficient mice develop systemic autoimmune phenotypes [17,29,30], making them a suitable model for studying such conditions. To further investigate the relationship between SIRT1 and autoimmunity, as well as the therapeutic potential of SIRT1 activation, we administered the SIRT1 agonists resveratrol (RSVL)—a natural polyphenol found in grapes and red wine [31] or SRT1720 to *Trex1-KO* mice daily for two weeks. Control animals received DMSO. Activation of SIRT1 significantly suppressed the expression of inflammatory mediators, including *Ifnb1*, *Oas1*, *Cxcl10*, and *Tnf* mRNA, compared to the DMSO-treated group (Fig. 9A–D). Furthermore, SIRT1 agonist treatment reduced immune cell infiltration into cardiac tissue (Fig. 9E). These findings highlight the potential utility of SIRT1 agonists in mitigating interferon-driven inflammation and autoimmunity, suggesting a promising therapeutic strategy for interferonopathies and related autoimmune diseases.

4. Discussion

Acetylation and deacetylation are critical modulators of innate immunity and inflammatory responses [6]. SIRT2 deacetylates cGAS and inhibit its activation [32]; while SIRT3 interacts with NLRC4 and deacetylates it at K71 or K272, enhancing NLRC4 inflammasome activation and promoting clearance of *S. typhimurium* [33]. SIRT1 has been shown to bind and deacetylate IFI16, inhibiting its cytoplasmic translocation and thereby attenuating host defenses against DNA viruses [34].

In this study, bioinformatics analysis revealed a negative correlation between SIRT1 expression and type I IFN signaling during influenza virus infection. Through dual-luciferase reporter, RT-qPCR, WB, fluorescence microscopy, etc. We demonstrated that SIRT1 inhibits virus-induced type I IFN signaling dependent on its deacetylase activity. Mechanistically, SIRT1 interacted with transcription factors IRF3 and IRF7, deacetylating IRF3 at K39/K77 and IRF7 at K92, without affecting their ubiquitination or dimerization. Notably, we report for the first time

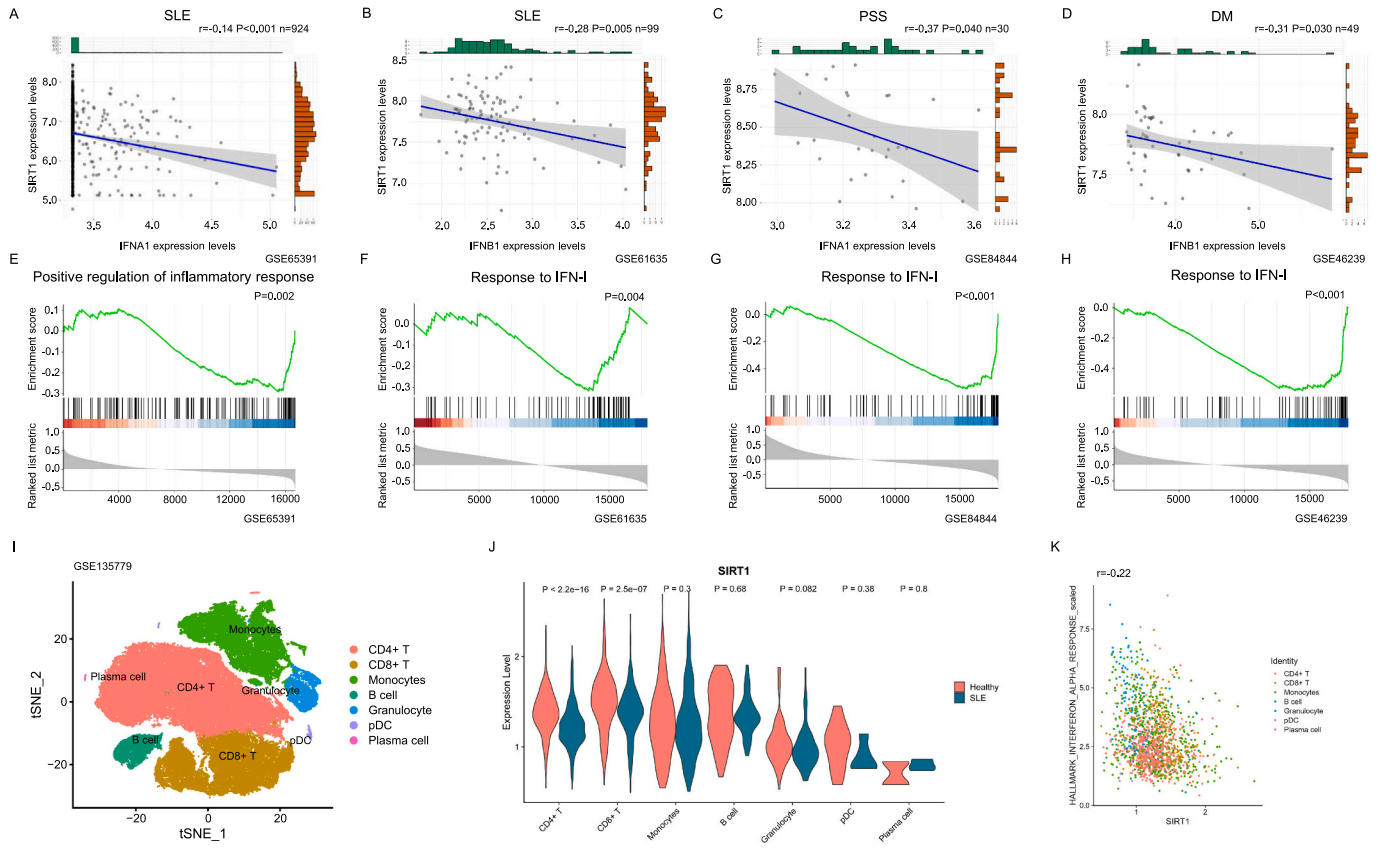

Fig. 8. SIRT1 is negatively correlated with autoimmune disease. A-D Correlation between the expression levels of *SIRT1* and *IFNA1/IFNB1* in the autoimmune disease groups of GSE65391 (A, $n = 924$), GSE61635 (B, $n = 99$), GSE84844 (C, $n = 30$), and GSE46239 (D, $n = 49$). *E*-H Analysis of the correlation between SIRT1 and the inflammatory response/IFN-I pathway through gene set enrichment analysis (GSEA) in GSE65391 (E), GSE61635 (F), GSE84844 (G), and GSE46239 (H). I t-SNE plot of major cell types identified in GSE135779. J SIRT1 expression of different cell types in GSE135779. K Correlation between the expression levels of SIRT1 and enrich score of IFN-I response gene sets in GSE135779.

that SIRT1 impedes the dephosphorylation of IRF3 at S97 and IRF7 at S101/S112 by the phosphatase PTENα, thereby blocking their nuclear translocation and suppressing IFN-I production.

Among IRF family members, IRF3 is the most extensively studied in the context of innate immunity. Phosphorylation at its C-terminal serine sites (S386 and S396) is essential for its full activation [21]. Similarly, IRF7 activation depends on phosphorylation at its C-terminal serine sites (e.g., S471/472, S477, S479, *etc.*), which are required for its nuclear translocation, DNA binding, and transcriptional activity [35–37]. In contrast, the functional significance of N-terminal phosphorylation in IRF3 and IRF7 remains poorly understood, and a role for SIRT1 in this process has not been previously explored.

Using IP technology and pan-phosphoserine antibody, we discovered that SIRT1 enhanced the phosphorylation level of the N-terminal domains of both IRF3 and IRF7, resulting in inhibition of IFN-I production. While IRF3 S97 phosphorylation is known to restrain nuclear translocation, and PTENα promotes antiviral responses by dephosphorylating this site [22]. One of the acetylation sites of the N-terminus of IRF3 is K77, which is also one of the key amino acids of the nuclear localization signal (NLS) of IRF3 [38,39]. Until now, the N-terminal phosphorylation of IRF7 and the exact nuclear localization signal of IRF7 remained unclear. We identified S101 and S112 within the N-terminal domain of IRF7 as novel phospho-sites negatively regulating its activity. Structural alignment revealed that S112 was evolutionarily analogous to IRF3 S97.

We further demonstrated that PTENα promotes IRF7 nuclear translocation by dephosphorylating its N-terminal region, while SIRT1 counteracts this process by deacetylating IRF7 at K92 and disrupting PTENα-mediated dephosphorylation. Although the nuclear localization signal of IRF7 has not been definitively mapped, predictive analyses suggest that K92—along with S101 and S112—resides near putative NLS regions, providing a structural rationale for their regulatory roles. Future studies are needed to experimentally validate the NLS of IRF7 and clarify the spatial and functional interplay between acetylation, phosphorylation, and nuclear transport.

Emerging evidence supports a negative regulatory function of SIRT1 in antiviral innate immunity. In a screening assay performed in murine BMDM, with knockdown of *Sirt1-Sirt7*, the expression of *Ifnβ* mRNA induced by RNA virus VSV is elevated after knockdown of *Sirt1* compared with the control group [40], aligning with our findings that SIRT1 suppresses the innate immune response to RNA viruses. Another study demonstrated that SIRT1 inhibits DNA virus-triggered antiviral innate immune response by deacetylating IFI16 and restraining its cytoplasmic localization [34], further corroborating our observation that SIRT1 also negatively modulates anti-DNA innate immune response. Recently, a study proposed that SIRT1 promotes virus-induced type I interferon production by deacetylating the DNA-binding domain (DBD) of IRF3/IRF7, thereby enhancing their liquid-liquid phase separation and association with ISRE-DNA in the nucleus [41]. Therefore, combining our data with reported literature, SIRT1 may exert bidirectional regulatory roles in antiviral innate immunity due to distinct variants, different subcellular localization, cell types, developmental stages or metabolic conditions. SIRT1 is also known to participate in diverse processes such as autophagy and metabolic regulation [42,43]. Under varying stress or nutrient availability, SIRT1 may fine-tune antiviral immune response through these ancillary pathways, underscoring the complexity of its immunoregulatory functions. Future studies should aim to elucidate how SIRT1 integrates metabolic, autophagic, and immune signals to precisely balance immune activation and

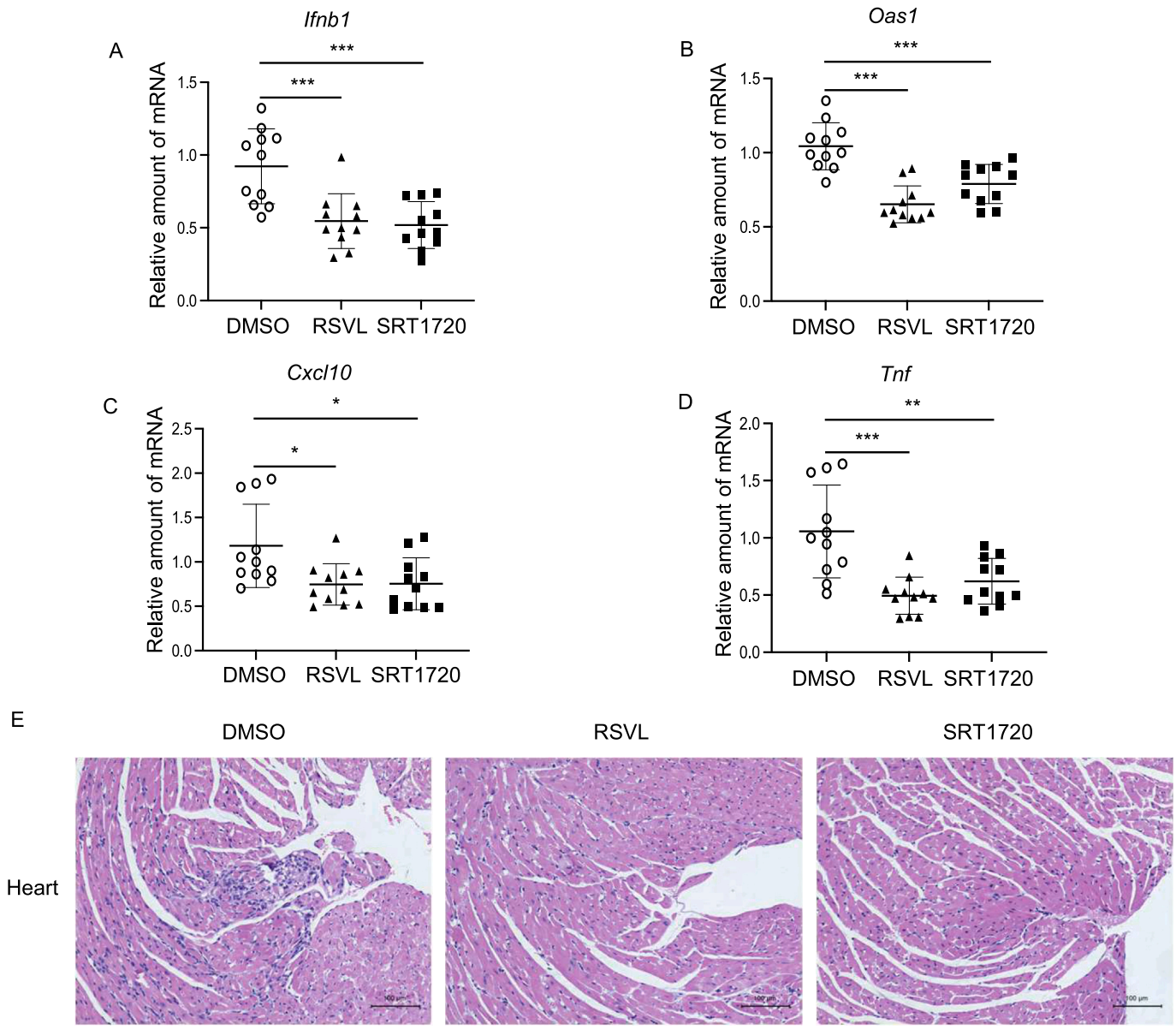

Fig. 9. SIRT1 agonists attenuated the spontaneous autoimmune phenotypes in Trex1-KO mice. A-D RT-qPCR analysis of *Ifnb1* (A), *Oas1* (B), *Cxcl10* (C), and *Tnf* (D) in the hearts of *Trex1-KO* mice ($n = 11$ per group) after being treated with DMSO or SIRT1 agonist RSVL (40 μg/g)/SRT1720 (20 μg/g) per day for 2 weeks. E HE staining of heart sections from mice in (I-L). (Scale bars, 100 μm, $^{*}P < 0.05$, $^{**}P < 0.01$, $^{***}P < 0.001$.)

suppression in a context-dependent manner.

The interplay between acetylation and other post-translational modifications (PTMs) represents a key mechanism for fine-tuning protein function. For instance, in colorectal cancer cells, dephosphorylation of ME1 at S336 by phosphatase PGAM5 facilitates subsequent acetylation at the adjacent K337 residue [44]. In this study, we uncover a novel regulatory axis wherein SIRT1-mediated deacetylation of the N-terminal domains of IRF3 and IRF7 impairs PTENα-dependent dephosphorylation, thereby suppressing their nuclear translocation.

In recent years, multiple novel PTMs have been identified, such as succinylation, crotonylation, lactonylation *etc.* [45–47]. Beyond deacetylation, the Sirtuin family is also involved in the removal of these novel PTMs [48–52]. For example, SIRT5 modulates antiviral immune response through its desuccinylase and demalonylase activities [40,53]. SIRT1 itself has been reported to remove crotonyl and lactyl groups [54–56], raising the possibility that it may regulate innate immunity through multiple catalytic activities beyond deacetylation.

It is also important to note that acetyltransferases and deacetylases often target a broad range of substrates, including histones and non-histone proteins [57]. Thus, SIRT1 may influence antiviral signaling not only through transcription factors like IRF3/IRF7 but also via histone modifications or as-yet-unidentified regulatory molecules. Future studies aimed at systematically identifying SIRT1 target modifications—including novel PTMs—will be essential to fully understand its multifaceted role in immune regulation.

Although IFN-I is known to have antiviral and antitumor effects, its chronic or dysregulated activation is strongly associated with the development of autoimmune disorders. Many autoimmune conditions (e.g., lupus, systemic sclerosis, desiccation syndrome, and dermatomyositis) are characterized by elevated IFN-I and ISGs in serum or tissues, which correlate with disease pathogenesis, clinical manifestations, and disease activity. Therapeutic therapies targeting the IFN-I pathway have demonstrated efficacy in both preclinical models and clinical trials [25]. The IFN-I blocking antibody anifrolumab was approved by the US FDA for the treatment of patients with SLE in 2021 [58,59], underscoring the significant clinical value of targeting this pathway. Our bioinformatic

analyses of autoimmune disease datasets revealed a negative correlation between *SIRT1* expression and levels of *IFNA1/IFNB1* genes as well as overall activation of the IFN-I signaling pathway, consistent with our experimental findings and supporting a potential protective role of SIRT1 in autoimmunity. Subsequent animal experiments using SIRT1 agonists (RSVL or SRT1720) lead to inhibition of expression of IFN-β and inflammatory cytokines, thus ameliorating autoimmune pathology in *Trex1-KO* mice. However, whether SIRT1 modulates the acetylation-phosphorylation crosstalk of IRF3/IRF7 in human autoimmune diseases remains to be experimentally validated.

Additional evidence supports the involvement of SIRT1 in autoimmune regulation. For instance, *Sirt1* null mice develop autoantibodies against nuclear antigens and exhibit immune complex deposition in the kidneys and liver [60]. The SIRT1 agonist RSVL ameliorates phenotypes in a pristane-induced lupus model [61]. In a Phase II trial (NCT01154101), SIRT1 agonist SRT2104 induced significant histological improvement in 35 % of patients with psoriasis [62]. However, despite the observed specificity towards SIRT1, both agents have been reported to exhibit multiple off-target activities [63,64]. Therefore, future studies should aim to confirm these findings using more selective SIRT1 activators.

Recent studies, including our own, have established that SIRT1 serves as a broad negative regulator of interferon signaling. We previously reported that SIRT1 inhibits both type I and type II IFN signaling by deacetylating STAT1 and STAT3, thereby attenuating JAK-STAT activation [16]. Furthermore, in *SIRT1-KO* A549-ACE2 cells, SARS-CoV-2 replication was significantly reduced [65]. Combining the current findings, these observations indicate that SIRT1 modulates multiple stages of antiviral immunity—both the production of IFN-I and the cellular response to IFNs. These insights provide a mechanistic basis for the therapeutic targeting of SIRT1 in viral infections, inflammatory disorders, and autoimmune diseases. For instance, SIRT1 inhibitors may enhance antiviral immunity, while SIRT1 agonists could mitigate pathological interferon activation in autoimmunity.

In summary, this study identified, for the first time, the negative regulatory role of N-terminal phosphorylation at S101/S112 on IRF7 modification for its activation and nuclear translocation. We also demonstrated that SIRT1-mediated deacetylation of the N-terminal domains of IRF3/IRF7 prevents PTENα-mediated dephosphorylation, thereby restraining their nuclear translocation, then blocking the functions of IRF3/IRF7. These findings not only deepen our understanding of IRF regulation and viral immune evasion strategies but also support the potential use of SIRT1 modulators—either agonists or antagonists—in the treatment of infections, inflammatory diseases, and interferonopathies.

CRediT authorship contribution statement

Shuang-Shuang Yu: Writing – original draft, Visualization, Formal analysis, Data curation, Conceptualization. **Hengxiang Yu:** Writing – original draft, Visualization, Formal analysis, Data curation, Conceptualization. **Shijin Geng:** Methodology, Investigation. **Rong-Chun Tang:** Validation. **Ao Zhang:** Validation. **Yan Zhang:** Resources. **Xiu-Yuan Sun:** Validation. **Jun Zhang:** Writing – review & editing, Supervision, Funding acquisition, Formal analysis, Data curation, Conceptualization.

Declaration of competing interest

The authors declare absence of any conflict of interest in the preparation, execution, and decision to publish of this study.

Acknowledgements

This study was supported by the National Natural Science Foundation of China (82271796 and 82071786) and Beijing Municipal Natural Science Foundation (M23006).

We thank Dr.Tomas Lindahl (The Francis Crick Institute, United Kingdom), Dr. Jianyuan Luo (Peking University, China), Dr. Tom Maniatis (Columbia University, USA), Dr. Takashi Fujita (Kyoto University, Japan), Dr. Hong-Bing Shu (Wuhan University, China), Dr. Zhijian J. Chen (University of Texas Southwestern Medical Center, USA), Dr. Wei Yu (Fudan University, China), Dr. Fuping You (Peking University, China), Dr. Zhenfang Jiang (Peking University, China),Dr. Hong Tang (Zhejiang University, China),Dr. Dan Lu (Peking University, China), for *Trex1*$^{+/-}$ mice, plasmids, cell line, or reagents. We thank Dr. Xin Zhang (Peking University, China) for instruction on bioinformatics analysis.

Appendix A. Supplementary data

Supplementary data to this article can be found online at https://doi.org/10.1016/j.ijbiomac.2025.147873.

Data availability

Data will be made available on request.

References

[1] R. Chen, J. Zou, J. Chen, X. Zhong, R. Kang, D. Tang, Pattern recognition receptors: function, regulation and therapeutic potential, Signal Transduct. Target. Ther. 10 (1) (2025) 216.
[2] T. Kawai, M. Ikegawa, D. Ori, S. Akira, Decoding toll-like receptors: recent insights and perspectives in innate immunity, Immunity 57 (4) (2024) 649–673.
[3] Z. Chen, R. Behrendt, L. Wild, M. Schlee, C. Bode, Cytosolic nucleic acid sensing as driver of critical illness: mechanisms and advances in therapy, Signal Transduct. Target. Ther. 10 (1) (2025) 90.
[4] S. Carpenter, L.A.J. O'Neill, From periphery to center stage: 50 years of advancements in innate immunity, Cell 187 (9) (2024) 2030–2051.
[5] J. Liu, C. Qian, X. Cao, Post-translational modification control of innate immunity, Immunity 45 (1) (2016) 15–30.
[6] J. Chen, D. Qi, H. Hu, X. Wang, W. Lin, Unconventional posttranslational modification in innate immunity, Cell. Mol. Life Sci. 81 (1) (2024) 290.
[7] M. Husain, Acetylation in viral infection and disease, Results Probl. Cell Differ. 75 (2025) 329–361.
[8] B. Hao, K. Chen, L. Zhai, M. Liu, B. Liu, M. Tan, Substrate and functional diversity of protein lysine post-translational modifications, Genomics Proteomics Bioinformatics 22 (1) (2024).
[9] J. Dai, Y.J. Huang, X. He, M. Zhao, X. Wang, Z.S. Liu, W. Xue, H. Cai, X.Y. Zhan, S. Y. Huang, K. He, H. Wang, N. Wang, Z. Sang, T. Li, Q.Y. Han, J. Mao, X. Diao, N. Song, Y. Chen, W.H. Li, J.H. Man, A.L. Li, T. Zhou, Z.G. Liu, X.M. Zhang, T. Li, Acetylation blocks cGAS activity and inhibits self-DNA-induced autoimmunity, Cell 176 (6) (2019) 1447–1460.e14.
[10] Z.M. Song, H. Lin, X.M. Yi, W. Guo, M.M. Hu, H.B. Shu, KAT5 acetylates cGAS to promote innate immune response to DNA virus, Proc. Natl. Acad. Sci. USA 117 (35) (2020) 21568–21575.
[11] H. Wang, Z. Cui, W. Sun, M. Yi, Y. Cheng, Y. Zhang, Y. Du, T. Pan, R. Gao, L. Feng, B. Zeng, G. Huang, Y. Li, Y. Wang, C.J. Zhang, R. He, C. Wang, MYO1F positions cGAS on the plasma membrane to ensure full and functional signaling, Mol. Cell 85 (1) (2025) 150–165.e7.
[12] M. Chen, J. Tan, Z. Jin, T. Jiang, J. Wu, X. Yu, Research progress on Sirtuins (SIRTs) family modulators, Biomed. Pharmacother. 174 (2024) 116481.
[13] Y. Yang, Y. Liu, Y. Wang, Y. Chao, J. Zhang, Y. Jia, J. Tie, D. Hu, Regulation of SIRT1 and its roles in inflammation, Front. Immunol. 13 (2022) 831168.
[14] H.J. Sun, S.P. Xiong, X. Cao, L. Cao, M.Y. Zhu, Z.Y. Wu, J.S. Bian, Polysulfide-mediated sulfhydration of SIRT1 prevents diabetic nephropathy by suppressing phosphorylation and acetylation of p65 NF-κB and STAT3, Redox Biol. 38 (2021) 101813.
[15] L.F. Chen, Y. Mu, W.C. Greene, Acetylation of RelA at discrete sites regulates distinct nuclear functions of NF-κB, EMBO J. 21 (23) (2002) 6539–6548.
[16] S.-S. Yu, R.-C. Tang, A. Zhang, S. Geng, H. Yu, Y. Zhang, X.-Y. Sun, J. Zhang, J.H. J. Ou, Deacetylase sirtuin 1 mitigates type I IFN- and type II IFN-induced signaling and antiviral immunity, J. Virol. 98 (3) (2024) e0008824.
[17] M. Morita, G. Stamp, P. Robins, A. Dulic, I. Rosewell, G. Hrivnak, G. Daly, T. Lindahl, D.E. Barnes, Gene-targeted mice lacking the Trex1 (DNase III) 3′–>5′ DNA exonuclease develop inflammatory myocarditis, Mol. Cell. Biol. 24 (15) (2004) 6719–6727.
[18] M.W. McBurney, X. Yang, K. Jardine, M. Hixon, K. Boekelheide, J.R. Webb, P. M. Lansdorp, M. Lemieux, The mammalian SIR2alpha protein has a role in embryogenesis and gametogenesis, Mol. Cell. Biol. 23 (1) (2003) 38–54.
[19] J.M. Solomon, R. Pasupuleti, L. Xu, T. McDonagh, R. Curtis, P.S. DiStefano, L. J. Huber, Inhibition of SIRT1 catalytic activity increases p53 acetylation but does not alter cell survival following DNA damage, Mol. Cell. Biol. 26 (1) (2006) 28–38.

[20] S. Broussy, H. Laaroussi, M. Vidal, Biochemical mechanism and biological effects of the inhibition of silent information regulator 1 (SIRT1) by EX-527 (SEN0014196 or selisistat), J. Enzyme Inhib. Med. Chem. 35 (1) (2020) 1124–1136.
[21] M. Al Hamrashdi, G. Brady, Regulation of IRF3 activation in human antiviral signaling pathways, Biochem. Pharmacol. 200 (2022) 115026.
[22] Y. Cao, H. Wang, L. Yang, Z. Zhang, C. Li, X. Yuan, L. Bu, L. Chen, Y. Chen, C.M. Li, D. Guo, PTEN-L promotes type I interferon responses and antiviral immunity, Cell. Mol. Immunol. 15 (1) (2018) 48–57.
[23] W. Ma, G. Huang, Z. Wang, L. Wang, Q. Gao, IRF7: role and regulation in immunity and autoimmunity, Front. Immunol. 14 (2023) 1236923.
[24] S. Shang, J. Liu, F. Hua, Protein acylation: mechanisms, biological functions and therapeutic targets, Signal Transduct. Target. Ther. 7 (1) (2022) 396.
[25] C.P. Mavragani, M.K. Crow, Type I interferons in health and disease: molecular aspects and clinical implications, Physiol. Rev. 105 (4) (2025) 2537–2587.
[26] Y.J. Crow, B.E. Hayward, R. Parmar, P. Robins, A. Leitch, M. Ali, D.N. Black, H. van Bokhoven, H.G. Brunner, B.C. Hamel, P.C. Corry, F.M. Cowan, S.G. Frints, J. Klepper, J.H. Livingston, S.A. Lynch, R.F. Massey, J.F. Meritet, J.L. Michaud, G. Ponsot, T. Voit, P. Lebon, D.T. Bonthron, A.P. Jackson, D.E. Barnes, T. Lindahl, Mutations in the gene encoding the 3′-5′ DNA exonuclease TREX1 cause Aicardi-Goutières syndrome at the AGS1 locus, Nat. Genet. 38 (8) (2006) 917–920.
[27] M.A. Lee-Kirsch, M. Gong, D. Chowdhury, L. Senenko, K. Engel, Y.A. Lee, U. de Silva, S.L. Bailey, T. Witte, T.J. Vyse, J. Kere, C. Pfeiffer, S. Harvey, A. Wong, S. Koskenmies, O. Hummel, K. Rohde, R.E. Schmidt, A.F. Dominiczak, M. Gahr, T. Hollis, F.W. Perrino, J. Lieberman, N. Hübner, Mutations in the gene encoding the 3′-5′ DNA exonuclease TREX1 are associated with systemic lupus erythematosus, Nat. Genet. 39 (9) (2007) 1065–1067.
[28] G.I. Rice, M.P. Rodero, Y.J. Crow, Human disease phenotypes associated with mutations in TREX1, J. Clin. Immunol. 35 (3) (2015) 235–243.
[29] J.L. Grieves, J.M. Fye, S. Harvey, J.M. Grayson, T. Hollis, F.W. Perrino, Exonuclease TREX1 degrades double-stranded DNA to prevent spontaneous lupus-like inflammatory disease, Proc. Natl. Acad. Sci. USA 112 (16) (2015) 5117–5122.
[30] N. Xiao, J. Wei, S. Xu, H. Du, M. Huang, S. Zhang, W. Ye, L. Sun, Q. Chen, cGAS activation causes lupus-like autoimmune disorders in a TREX1 mutant mouse model, J. Autoimmun. 100 (2019) 84–94.
[31] A.P. Singh, R. Singh, S.S. Verma, V. Rai, C.H. Kaschula, P. Maiti, S.C. Gupta, Health benefits of resveratrol: evidence from clinical studies, Med. Res. Rev. 39 (5) (2019) 1851–1891.
[32] M. Barthez, B. Xue, J. Zheng, Y. Wang, Z. Song, W.C. Mu, C.L. Wang, J. Guo, F. Yang, Y. Ma, X. Wei, C. Ye, N. Sims, L. Martinez-Sobrido, S. Perlman, D. Chen, SIRT2 suppresses aging-associated cGAS activation and protects aged mice from severe COVID-19, Cell Rep. 44 (4) (2025) 115562.
[33] C. Guan, X. Huang, J. Yue, H. Xiang, S. Shaheen, Z. Jiang, Y. Tao, J. Tu, Z. Liu, Y. Yao, W. Yang, Z. Hou, J. Liu, X.-D. Yang, Q. Zou, B. Su, Z. Liu, J. Ni, J. Cheng, X. Wu, SIRT3-mediated deacetylation of NLRC4 promotes inflammasome activation, Theranostics 11 (8) (2021) 3981–3995.
[34] J. Wang, X. Qin, Y. Huang, G. Zhang, Y. Liu, Y. Cui, Y. Wang, J. Pei, S. Ma, Z. Song, X. Zhu, H. Wang, B. Yang, J.U. Jung, Sirt1 negatively regulates cellular antiviral responses by preventing the cytoplasmic translocation of interferon-inducible protein 16 in human cells, J. Virol. 97 (2) (2023) e0197522.
[35] R. Lin, Y. Mamane, J. Hiscott, Multiple regulatory domains control IRF-7 activity in response to virus infection, J. Biol. Chem. 275 (44) (2000) 34320–34327.
[36] A. Caillaud, A.G. Hovanessian, D.E. Levy, I.J. Marié, Regulatory serine residues mediate phosphorylation-dependent and phosphorylation-independent activation of interferon regulatory factor 7, J. Biol. Chem. 280 (18) (2005) 17671–17677.
[37] H. Yang, C.H. Lin, G. Ma, M.O. Baffi, M.G. Wathelet, Interferon regulatory factor-7 synergizes with other transcription factors through multiple interactions with p300/CBP coactivators, J. Biol. Chem. 278 (18) (2003) 15495–15504.
[38] K.P. Kumar, K.M. McBride, B.K. Weaver, C. Dingwall, N.C. Reich, Regulated nuclear-cytoplasmic localization of interferon regulatory factor 3, a subunit of double-stranded RNA-activated factor 1, Mol. Cell. Biol. 20 (11) (2000) 4159–4168.
[39] M. Zhu, T. Fang, S. Li, K. Meng, D. Guo, Bipartite nuclear localization signal controls nuclear import and DNA-binding activity of IFN regulatory factor 3, J. Immunol. 195 (1) (2015) 289–297.
[40] X. He, T. Li, K. Qin, S. Luo, Z. Li, Q. Ji, H. Song, H. He, H. Tang, C. Han, H. Li, Y. Luo, Demalonylation of DDX3 by Sirtuin 5 promotes antiviral innate immune responses, Theranostics 11 (15) (2021) 7235–7246.
[41] Z. Qin, X. Fang, W. Sun, Z. Ma, T. Dai, S. Wang, Z. Zong, H. Huang, H. Ru, H. Lu, B. Yang, S. Lin, F. Zhou, L. Zhang, Deactylation by SIRT1 enables liquid-liquid phase separation of IRF3/IRF7 in innate antiviral immunity, Nat. Immunol. 23 (8) (2022) 1193–1207.
[42] J.Y. Kim, D. Mondaca-Ruff, S. Singh, Y. Wang, SIRT1 and autophagy: implications in endocrine disorders, Front. Endocrinol. (Lausanne) 13 (2022) 930919.
[43] Y. Chen, H. Yang, S. Chen, Z. Lu, B. Li, T. Jiang, M. Xuan, R. Ye, H. Liang, X. Liu, Q. Liu, H. Tang, SIRT1 regulated hexokinase-2 promoting glycolysis is involved in hydroquinone-enhanced malignant progression in human lymphoblastoid TK6 cells, Ecotoxicol. Environ. Saf. 241 (2022) 113757.
[44] Y. Zhu, L. Gu, X. Lin, C. Liu, B. Lu, K. Cui, F. Zhou, Q. Zhao, E.V. Prochownik, C. Fan, Y. Li, Dynamic regulation of ME1 phosphorylation and acetylation affects lipid metabolism and colorectal tumorigenesis, Mol. Cell 77 (1) (2020) 138–149.e5.
[45] G. Millán-Zambrano, A. Burton, A.J. Bannister, R. Schneider, Histone post-translational modifications - cause and consequence of genome function, Nat. Rev. Genet. 23 (9) (2022) 563–580.
[46] M. Tan, H. Luo, S. Lee, F. Jin, J.S. Yang, E. Montellier, T. Buchou, Z. Cheng, S. Rousseaux, N. Rajagopal, Z. Lu, Z. Ye, Q. Zhu, J. Wysocka, Y. Ye, S. Khochbin, B. Ren, Y. Zhao, Identification of 67 histone marks and histone lysine crotonylation as a new type of histone modification, Cell 146 (6) (2011) 1016–1028.
[47] D. Zhang, Z. Tang, H. Huang, G. Zhou, C. Cui, Y. Weng, W. Liu, S. Kim, S. Lee, M. Perez-Neut, J. Ding, D. Czyz, R. Hu, Z. Ye, M. He, Y.G. Zheng, H.A. Shuman, L. Dai, B. Ren, R.G. Roeder, L. Becker, Y. Zhao, Metabolic regulation of gene expression by histone lactylation, Nature 574 (7779) (2019) 575–580.
[48] J. Jin, L. Bai, D. Wang, W. Ding, Z. Cao, P. Yan, Y. Li, L. Xi, Y. Wang, X. Zheng, H. Wei, C. Ding, Y. Wang, SIRT3-dependent delactylation of cyclin E2 prevents hepatocellular carcinoma growth, EMBO Rep. 24 (5) (2023) e56052.
[49] J. Du, Y. Zhou, X. Su, J.J. Yu, S. Khan, H. Jiang, J. Kim, J. Woo, J.H. Kim, B. H. Choi, B. He, W. Chen, S. Zhang, R.A. Cerione, J. Auwerx, Q. Hao, H. Lin, Sirt5 is a NAD-dependent protein lysine demalonylase and desuccinylase, Science 334 (6057) (2011) 806–809.
[50] S. Sadhukhan, X. Liu, D. Ryu, O.D. Nelson, J.A. Stupinski, Z. Li, W. Chen, S. Zhang, R.S. Weiss, J.W. Locasale, J. Auwerx, H. Lin, Metabolomics-assisted proteomics identifies succinylation and SIRT5 as important regulators of cardiac function, Proc. Natl. Acad. Sci. USA 113 (16) (2016) 4320–4325.
[51] A.Q. Yu, J. Wang, S.T. Jiang, L.Q. Yuan, H.Y. Ma, Y.M. Hu, X.M. Han, L.M. Tan, Z. X. Wang, SIRT7-induced PHF5A decrotonylation regulates aging progress through alternative splicing-mediated downregulation of CDK2, Front. Cell Dev. Biol. 9 (2021) 710479.
[52] H.B. Yu, S.T. Cheng, F. Ren, Y. Chen, X.F. Shi, V.K.W. Wong, B.Y.K. Law, J.H. Ren, S. Zhong, W.X. Chen, H.M. Xu, Z.Z. Zhang, J.L. Hu, X.F. Cai, Y. Hu, W.L. Zhang, Q. X. Long, L. He, Z.W. Hu, H. Jiang, H.Z. Zhou, A.L. Huang, J. Chen, SIRT7 restricts HBV transcription and replication through catalyzing desuccinylation of histone H3 associated with cccDNA minichromosome, Clin. Sci. (Lond.) 135 (12) (2021) 1505–1522.
[53] X. Liu, C. Zhu, H. Zha, J. Tang, F. Rong, X. Chen, S. Fan, C. Xu, J. Du, J. Zhu, J. Wang, G. Ouyang, G. Yu, X. Cai, Z. Chen, W. Xiao, SIRT5 impairs aggregation and activation of the signaling adaptor MAVS through catalyzing lysine desuccinylation, EMBO J. 39 (11) (2020) e103285.
[54] X. Bao, Y. Wang, X. Li, X.M. Li, Z. Liu, T. Yang, C.F. Wong, J. Zhang, Q. Hao, X. D. Li, Identification of 'erasers' for lysine crotonylated histone marks using a chemical proteomics approach, Elife 3 (2014).
[55] S. Hao, Y. Wang, Y. Zhao, W. Gao, W. Cui, Y. Li, J. Cui, Y. Liu, L. Lin, X. Xu, H. Wang, Dynamic switching of crotonylation to ubiquitination of H2A at lysine 119 attenuates transcription-replication conflicts caused by replication stress, Nucleic Acids Res. 50 (17) (2022) 9873–9892.
[56] C. Moreno-Yruela, D. Zhang, W. Wei, M. Bæk, W. Liu, J. Gao, D. Danková, A. L. Nielsen, J.E. Bolding, L. Yang, S.T. Jameson, J. Wong, C.A. Olsen, Y. Zhao, Class I histone deacetylases (HDAC1-3) are histone lysine delactylases, Sci. Adv. 8 (3) (2022) eabi6696.
[57] M. Shvedunova, A. Akhtar, Modulation of cellular processes by histone and non-histone protein acetylation, Nat. Rev. Mol. Cell Biol. 23 (5) (2022) 329–349.
[58] M. Ramaswamy, R. Tummala, K. Streicher, A. Nogueira da Costa, P.Z. Brohawn, The pathogenesis, molecular mechanisms, and therapeutic potential of the interferon pathway in systemic lupus erythematosus and other autoimmune diseases, Int. J. Mol. Sci. 22 (20) (2021).
[59] A. Psarras, M. Wittmann, E.M. Vital, Emerging concepts of type I interferons in SLE pathogenesis and therapy, Nat. Rev. Rheumatol. 18 (10) (2022) 575–590.
[60] J. Sequeira, G. Boily, S. Bazinet, S. Saliba, X. He, K. Jardine, C. Kennedy, W. Staines, C. Rousseaux, R. Mueller, M.W. McBurney, sirt1-null mice develop an autoimmune-like condition, Exp. Cell Res. 314 (16) (2008) 3069–3074.
[61] Z.-L. Wang, X.-F. Luo, M.-T. Li, D. Xu, S. Zhou, H.-Z. Chen, N. Gao, Z. Chen, L.-L. Zhang, X.-F. Zeng, Resveratrol possesses protective effects in a pristane-induced lupus m ouse model, PLoS One 9 (12) (2014) e114792.
[62] J.G. Krueger, M. Suárez-Fariñas, I. Cueto, A. Khacherian, R. Matheson, L.C. Parish, C. Leonardi, D. Shortino, A. Gupta, J. Haddad, G.P. Vlasuk, E.W. Jacobson, A randomized, placebo-controlled study of SRT2104, a SIRT1 activator, in patients with moderate to severe psoriasis, PLoS One 10 (11) (2015) e0142081.
[63] M. Gertz, G.T.T. Nguyen, F. Fischer, B. Suenkel, C. Schlicker, B. Fränzel, J. Tomaschewski, F. Aladini, C. Becker, D. Wolters, C. Steegborn, A molecular mechanism for direct sirtuin activation by resveratrol, PLoS One 7 (11) (2012) e49761.
[64] M. Pacholec, J.E. Bleasdale, B. Chrunyk, D. Cunningham, D. Flynn, R.S. Garofalo, D. Griffith, M. Griffor, P. Loulakis, B. Pabst, X. Qiu, B. Stockman, V. Thanabal, A. Varghese, J. Ward, J. Withka, K. Ahn, SRT1720, SRT2183, SRT1460, and resveratrol are not direct activators o f SIRT1, J. Biol. Chem. 285 (11) (2010) 8340–8351.
[65] M. Walter, I.P. Chen, A. Vallejo-Gracia, I.J. Kim, O. Bielska, V.L. Lam, J. M. Hayashi, A. Cruz, S. Shah, F.W. Soveg, J.D. Gross, N.J. Krogan, K.R. Jerome, B. Schilling, M. Ott, E. Verdin, SIRT5 is a proviral factor that interacts with SARS-CoV-2 Nsp14 protein, PLoS Pathog. 18 (9) (2022) e1010811.